A STUDY OF THE METHANATION OF A FLOWING H_2 - CO GAS MIXTURE IN A PLASMA CATALYZED REACTOR

PART I - THE METHANATION OF A FLOWING H_2 - CO GAS MIXTURE IN A PLASMA CATALYZED REACTOR

PART II - THE MICROWAVE PLASMA AS CATALYST IN THE METHANATION STEP

Thesis for the Degree of M. S.

MICHIGAN STATE UNIVERSITY

RICHARD L. HOLLOWAY

1973

ABSTRACT

THE METHANATION OF A FLOWING H_2 - CO GAS MIXTURE
IN A PLASMA CATALYZED REACTOR

By

Richard L. Holloway

Mixtures of H_2 - CO were continuously pasted through a microwave plasma in a quartz tubular reactor. Conversions up to 25% were obtained for residence times of 0.07 to 1.5 seconds and pressures of 2 to 50 mmHg. CH_4 conversions increased with increasing H_2 concentration, with a 4:1 volumetric ratio giving the highest yield under the experimental operating conditions. The power that gave the highest yield to CH_4 was 250 to 600 watts, with thermal decomposition of hydrocarbons occurring at higher power levels. Approximately 150 watts were required to maintain the microwave plasma. CH≡CH was identified as the major biproduct, and a mechanism incorporating a (CH•) intermediate is postulated to account for the two hydrocarbon products.

A STUDY OF THE METHANATION OF A FLOWING H_2 - CO GAS MIXTURE IN A PLASMA CATALYZED REACTOR

PART I - THE METHANATION OF A FLOWING H_2 - CO GAS MIXTURE IN A PLASMA CATALYZED REACTOR

PART II - THE MICROWAVE PLASMA AS CATALYST IN THE METHANATION STEP

By

Richard L. Holloway

A THESIS

Submitted to
Michigan State University
in partial fulfillment of the requirements
for the degree of

MASTER OF SCIENCE

Department of Chemical Engineering

1973

ACKNOWLEDGMENTS

The author gratefully acknowledges the Detroit Edison Company and the Division of Engineering Research at Michigan State University for their financial support of this work.

Appreciation is extended to Dr. M. C. Hawley, Dr. B. W. Wilkinson, and Dr. J. Asmussen for their technical assistance and guidance during the course of the project.

TABLE OF CONTENTS

LIST OF FIGURES

LIST OF TABLES

INTRODUCTION

Many chemical reactions in electric discharge or plasma have been studied over the past twenty years,[1,2,3,4,8] the majority of these being in batch systems. However, never has the need been greater to pursue the possibility of production of synthetic natural gas from coal in a continuous flowing plasma reactor. In view of the critical supply and demand situation for energy in this country and the increasing concern on environmental quality it is essential that new coal processing techniques be investigated through engineering research and development. This study is a report and analysis of the first results of the research effort at Michigan State University to produce methane from CO and H_2 via microwave catalysis. The system for methanation experiments consisted of a flowing H_2 - CO gas mixture through a microwave field to produce the catalysis effect. It should be emphasize that the project although speculative in nature entails a unique, unexplored area in both plasma optimization and chemical process development.

The overall research project is broken down into separate studies of the methanation in a plasma reactor, gasification in a plasma, hydrogenation of coal in a plasma, and finally the ultimate goal of a combined methanation and gasification process. Preliminary economics for a plasma system have been developed by Asmussen, Hawley, and Wilkinson in the original Michigan State University research proposal.[14] Their speculative economics indicated a potential 15% savings in capital investment and a

10% decrease in operating cost. Further experimental work will establish a firmer base case for preliminary design and comparison with other schemes in coal processing.

The two routes for producing SNG (high Btu gas) which are being developed and commercialized are 1) SNG from naphtha and 2) SNG from coal. Both schemes are similar in chemistry; i.e., both require gasification, shift, and methanation. The chemical reactions for these steps are written for SNG from coal as follows:

(a) Gasification

$$2C + 2H_2O \rightarrow 2CO + 2H_2$$

(b) Shift

$$CO + H_2O \rightarrow CO_2 + H_2$$

(c) Methanation

$$3H_2 + CO \xrightarrow[\text{catalyst}]{\text{nickel}} CH_4 + H_2O$$

The net process can be summarized as

$$2C + 2H_2O \rightarrow CH_4 + CO_2$$

A unique feature of the project is that the microwave source provides only the energy to maintain the plasma for catalysis of the methanation reaction. This will also be the case in future work on a plasma reactor which will carry out both the gasification and methanation reactions in a single unit, thus eliminating a portion of the costly process equipment of the current SNG routes.

Many investigators have studied the production of hydrocarbons in electric discharges and there have been several H_2 - CO - CO_2 studies in microwave,[5,6] megahertz,[7] and corona discharges.[8,9] One of particular interest is by Epple and Apt[7] who have shown it possible to convert

mixtures of H_2 and CO_2 to methane in electrical discharges ranging in frequency from 2-110 megacycles. Their work was performed in a static system with residence times of 2-3 minutes and reported conversions as high as 55% of the total input of carbon to CH_4.

PART I - THE METHANATION OF A FLOWING H_2 - CO GAS MIXTURE IN A PLASMA CATALYZED REACTOR

MATERIAL AND EQUIPMENT

The process flow diagram is shown in Figure 1. A 5 ft^3 cylinder was used for the premix tank, with a gas regulator that gave a constant discharge pressure of 5 psig. The premix tank was evacuated and then flushed several times with H_2 to remove any oxygen that might have been in tank after use. Oxygen being a free radical acceptor must be completely eliminated in order to achieve the methanation step. The feed gases are then passed over a $CaSO_4$ packed bed to insure the removal of any H_2O since this drives the methanation reaction in the reverse direction. Flow rates are then measured using a rotameter with a selection of rotameter tubes that allowed a flow range of 5-10,000 cc/min at S.T.P. The gases were preheated in some experiments using a high voltage-low amp electrical source which conducted a current through a 30' section of 1/32" OD pipe.

The reactor system consists of a 12" diameter cavity with cooling coils around the outer perimeter and 1/64" holes for electric field strength probes (Figure 3). As the hot gases leave the preheater they enter the 1" OD quartz tube where the plasma is generated and the reaction takes place. Reactor discharge gases are then passed through a two stage cooling system, the first a dry ice-ethylene gycol solution (-30°F) and then a water bath. This cooling section may be bypassed if sufficient natural convection occurs from the reactor outlet to the cooling system from the pipe. A final drying bed of $CaSO_4$ is utilized to remove any traces

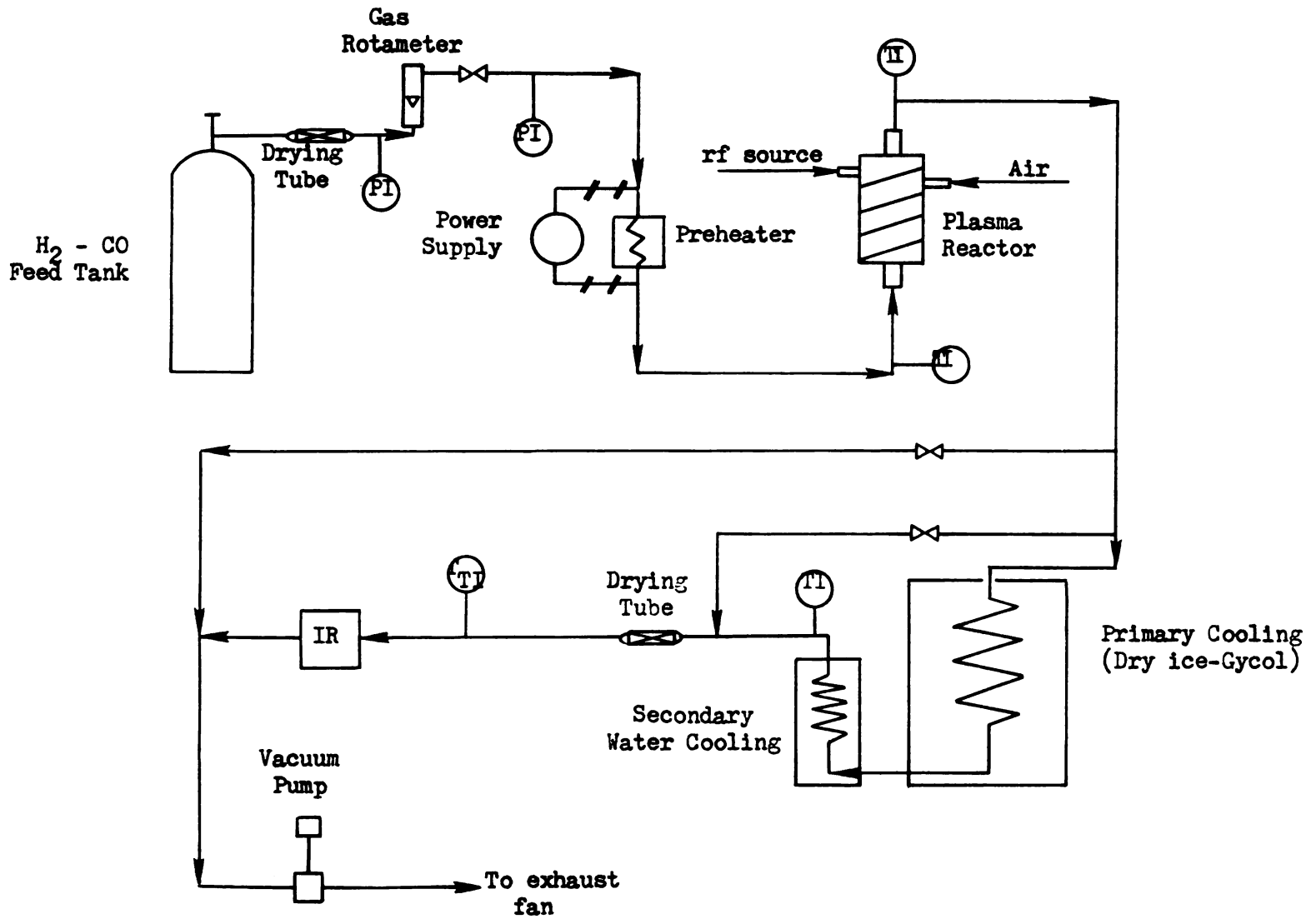

Figure 1. Process flow diagram for Plasma catalyzed Methanation.

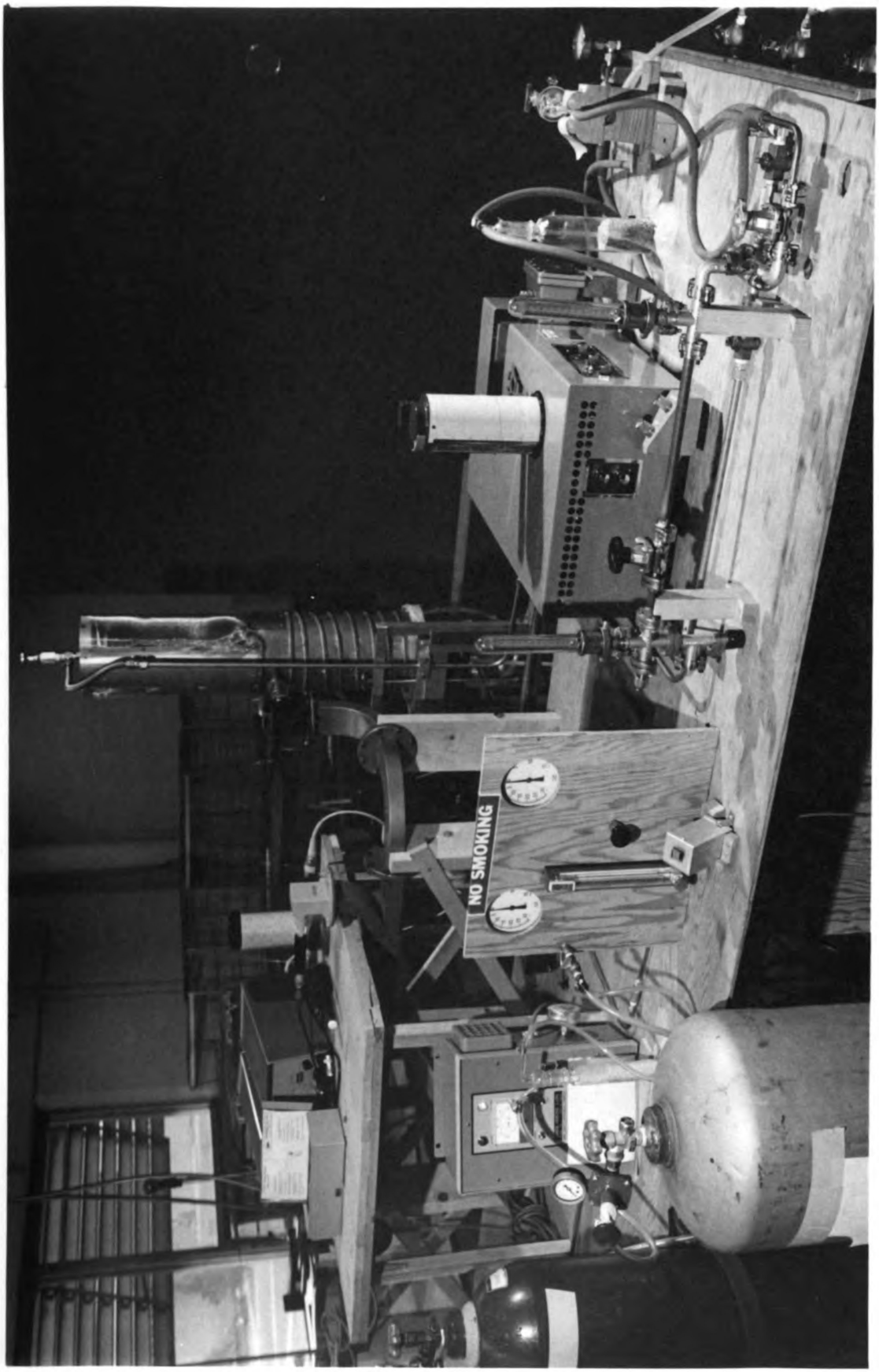

Figure 2 . Chemical processing equipment

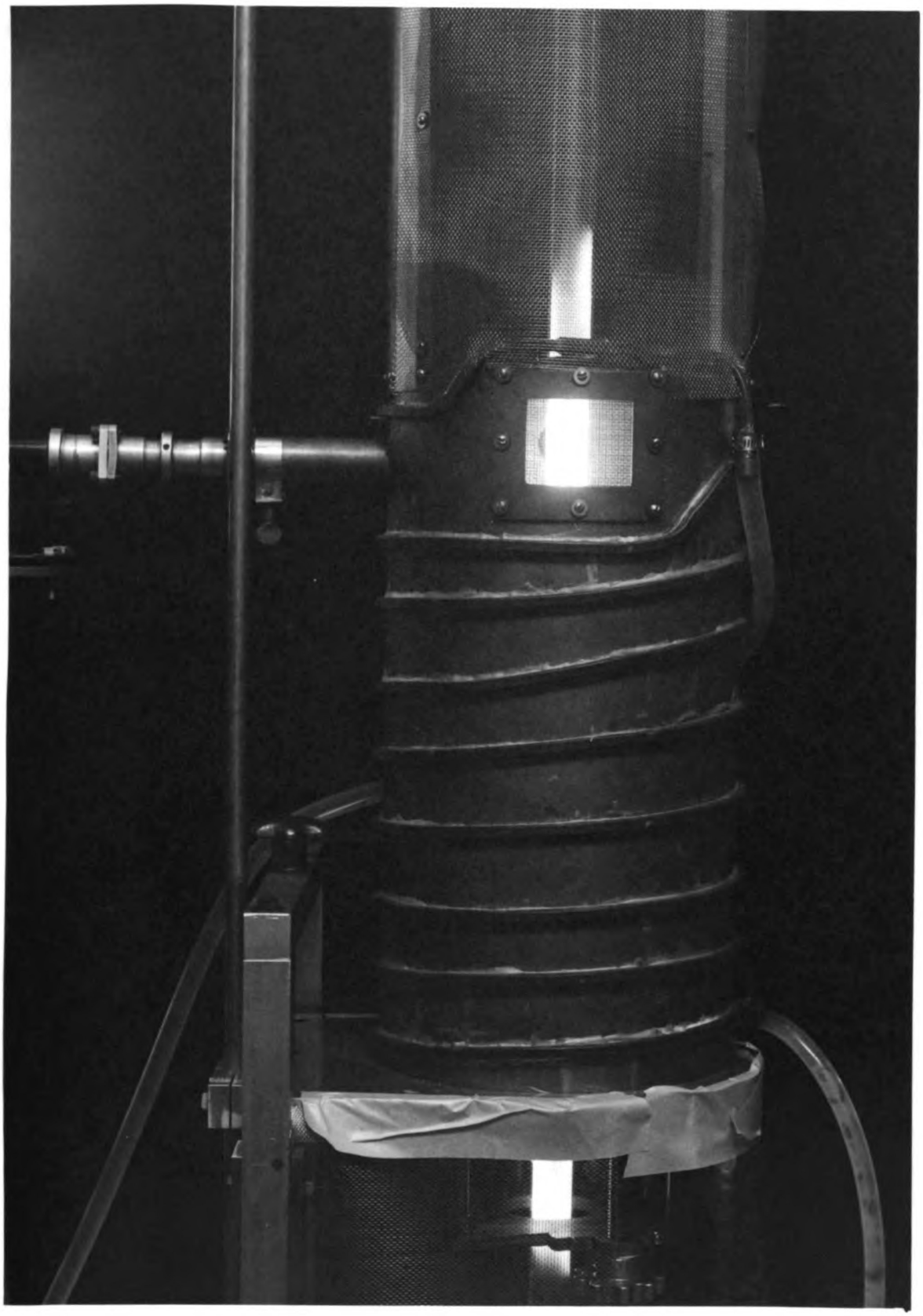

Figure 3 . rf plasma reactor

of water produced from the reaction. Water absorbs in the same region as CH_4 in the IR so must be removed. The IR analysis was done with a Perkin-Elmer spectrophotometer utilizing a 1 meter gas cell. A reference cell was also used. After the gases were analyzed they were drawn through the vacuum pump and discharge to an exhaust fan.

Instrumentation consisted of temperature and pressure gages located about the reactor and cooling system, along with sample points for mass spectra. Piping up to the preheater was 1/4" OD copper tubing while 1/2" OD stainless steel was used after the preheater. Due to the extremely toxic nature of the CO, a MSA carbon monoxide detector was used during all work. A safety shield enclosed the reactor as an explosion protection device.

During the course of the experimental work the following mechanical or process problems were encountered.

Problem: The entire system had to be vacuum tight with a leakage rate of less than 2 cc/min of air.

Action: All connections were sealed with gyptol or high vacuum grease.

Problem: High power inputs caused the deposition of carbon on the walls and the quartz reactor tube to melt.

Action: Provided an air cooling system in the reactor cavity and changed the power divider to reduce power input.

Problem: Preheater was fabricated with stainless steel tubes containing nickel which at higher pressures could produce CH_4 due to the catalysis effect.

Action: Nickel in tubes was poisoned using sulfur dioxide.

Problem: Temperature measurement of gases under high vacuum.

Action: An infrared pyrometer was tested.

Problem: Excessive dust from drying tube collected on I.R. cell mirrors.

Action: Glass wool filter was installed after drying tube.

EXPERIMENTAL PROCEDURE

The complete system is first evacuated to less than 1 mm Hg. The H_2 - CO feed valve is opened to establish a flowing system under high vacuum and purge out any remaining air. As an initial start-up step, the rotameter flow is set to 100 cc/min of H_2 - CO mixture and a pressure of 2 mm Hg. The microwave rf source is turned on and the sliding short adjusted to produce enough power to create the necessary ionization required to establish a plasma. The cavity (plasma) length is then adjusted in order to optimize or retune the plasma. Once the plasma is generated the pressure is increased step wise, each time adjusting the sliding short and cavity length (see Part II. Microwave Plasma Reactor Design for mechanical details). When the system has reached steady state, the reactor discharge is analyzed on the Infrared Spectrophotometer by scanning the 4000-1300 cm^{-1} region. The appropriate variables are recorded and the system changed to a new set of parameters.

MODEL OF SYSTEM AND DEFINITIONS

Consider a H_2 - CO gas mixture flowing through a tubular reactor with a microwave plasma being generated inside the tube producing a chemical reaction. This is illustrated below along with the associated variables. The objective of the plasma catalyzed reactor is to maximize conversion to methane by the following reaction, while

(1) $3H_2 + CO \longrightarrow CH_4 + H_2O$

minimizing power requirements and biproduct formation.

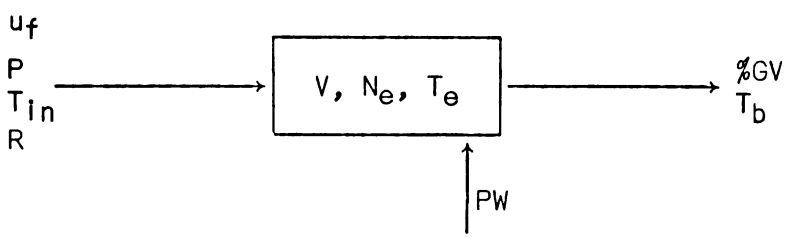

T_{in} - inlet temperature

P - system pressure

u_f - volumetric flow rate of H_2 - CO mixture which is a function of the system pressure, $\underline{P}$, and inlet temperature, $\underline{T_{in}}$.

R - ratio of H_2/CO

V - reactor volume dependent on the cavity length

PW - power absorbed in cavity

N_e - electron density which is a function of pressure, $\underline{P}$, and power absorbed, $\underline{PW}$

T_e - electron temperature in reactor which is dependent on electron density, $\underline{N_e}$, and power, $\underline{PW}$

T_b - bulk temperature of gas leaving plasma reactor

%GV - percent by volume of hydrocarbon product in reactor discharge which is a function of the following,

1) Temperature, $\underline{T_b}$, and $\underline{T_e}$
2) Pressure, $\underline{P}$
3) Electron density, $\underline{N_e}$
4) Volumetric flow rate, $\underline{u_f}$, and ratio of H_2/CO, $\underline{R}$
5) Power absorbed in cavity, $\underline{PW}$

If we assume no volume change occurs in the reactor the design equation for the system is shown in equation (2).

$$(2) \quad \frac{V}{u_f} = \int \frac{d(CH_4)}{r(T_b, T_e, P, N_e, R)}$$

where (CH_4) = methane concentration
r = rate of reaction of reactants

RESULTS AND DISCUSSION

The first methanation experiments shown in Table 1 (runs 13001-20104) had flow rates of 1000-3000 cc/min producing very small residence times in the plasma reactor. All previous work[5,7] in this area had been on static systems using very high residence times of 2-3 minutes, however in the initial work on the economics of the project residence times of less than 2 seconds were necessary to establish satisfactory power savings. The power levels were above 1500 watts which created a plasma with a reddish glow that completely filled the quartz tube in the cavity. There was no basis for starting at these power levels, except providing enough power to produce the plasma in the flowing H_2 - CO system. The first H_2 - CO feed tried was a 10:1 mixture (by volume) of hydrogen rich gas. Since previous experimental work on hydrogen in a microwave plasma had been conducted by Asmussen,[10,11] one of the principal investigators, the initial generation of the plasma was done in a hydrogen rich feed. The TE011 mode was the resonant frequency used in these runs corresponding to a cavity length of 9.8 cm.

The flowing gases were analyzed on the IR spectrophotometer in these runs, however, they showed no methane bands. Also mass spectra samples gave negative results. However, a very significant finding of these runs (13001-20104) was the observation of a carbon deposition on the quartz tube wall. This certainly indicated the presence of a chemical reaction occurring in the flowing gas mixture. Figure 4, for the

Table 1. Experimental Data

run number	feed ratio H_2/CO	gas flow[1] cc/min	pres. mmHg	cavity length, cm	mode[4]	power[3] watts	resi-dence[2] time, sec	% volume CH_4	IR curve number	Remarks
13001	10/1	1000	15	9.8	TE011	1200	.030	0.0	- -	IR and mass spectra showed (no CH_4 or acetylene)
13002	10/1	3000	35	9.8	TE011	1105	.022	"	- -	
13003	10/1	1000	50	9.8	"	1050	0.10	"	- -	carbon deposits forming on tube walls
13004	10/1	1000	50	9.8	"	980	0.10	"	- -	
20101	10/1	1500	15	9.8	"	1200	.02	"	- -	
20102	10/1	1000	25	9.8	"	1080	.050	"	- -	
20103	10/1	1000	35	9.8	"	940	0.068	0.0	- -	
20104	10/1	1000	50	9.8	TE011	940	0.098	0.0	- -	hotspots formed, quartz tube melted
30101	4/1	100	13	13.9	TE*112	70	.35	0.85	2	first observed CH_4 formation
30102	4/1	100	20	13.9	TE*112	250	.55	0.11	"	
30103	4/1	"	30	13.9	TE*112	- -	.825	0.67	"	
30104	4/1	"	39	"	"	240	1.07	1.52	"	
30105	4/1	"	48	"	"	60	1.32	0.53	"	
30106	4/1	"	48	"	"	160	1.32	0.74	"	
30107	4/1	"	55	"	"	210	1.51	0.35	"	quartz tube shows hots spots on walls

Table 1. Experimental Data (continued)

run number	feed ratio H_2/CO	gas flow[1] cc/min	pres. mmHg	cavity length, cm	mode[4]	power[3] watts	resi-dence[2] time, sec	% volume CH_4	IR curve number	Remarks
30108	4/1	100	39	13.9	TE*112	270	1.08	- -	2	% transmittance on IR to low for recording
30109	4/1	"	15	"	"	280	.41	- -	"	
30110	4/1	"	10	"	"	290	.27	- -	"	
30111	4/1	"	10	"	"	250	.27	- -	"	
30112	4/1	"	12	"	"	160	.30	- -	"	
30113	4/1	100	12	13.9	TE*112	105	.30	- -	2	
30601	4/1	70	15	13.8	TE*112	299	.58	2.17	5	
30602	4/1	35	15	13.8	"	289	1.17	1.30	5	
30603	4/1	83	15	"	"	276	.40	1.74	6	
30604	4/1	115	15	"	"	873	.35	.22	6	
30605	4/1	115	15	"	"	263	.35	1.08	6	
30606	4/1	115	15	"	"	368	.35	1.08	6	
30607	4/1	115	15	"	"	210	.35	.87	6	
30608	4/1	83	25	"	"	527	.82	.87	6	
30609	4/1	83	25	"	"	409	.82	.87	6	

Table 1. Experimental Data (continued)

run number	feed ratio H_2/CO	gas flow[1] cc/min	pres. mmHg	cavity length, cm	mode[4]	power[3] watts	resi-dence[2] time, sec	% volume CH_4	IR curve number	Remarks
30610	4/1	83	25	13.8	TE*112	256	0.82	0.43	6	
30611	4/1	83	25	"	"	418	0.82	0.43	6	
30701	4/1	83	2	"	"	690	.07	5.4	8	
30702	4/1	83	2	"	"	331	.07	5.4	8	
30703	4/1	83	2	"	"	140	.07	0.0	8	
30704	4/1	83	2	"	"	337	.07	0.0	8	
30705	4/1	83	10	"	"	386	.33	2.17	8	
30706	4/1	83	10	"	"	890	.33	0.0	8	
30707	4/1	83	25	"	"	557	.8	1.08	8	
30708	4/1	83	40	"	"	553	1.3	1.08	8	
30709	4/1	60	40	"	"	545	1.8	0.54	8	
30710	4/1	115	40	"	"	545	0.9	0.43	8	
30711	4/1	83	40	"	"	545	1.3	0.98	9	
30712	4/1	83	40	"	"	646	1.3	0.98	9	
30713	4/1	83	40	"	"	746	1.3	0.98	9	

Table 1. Experimental Data (continued)

run number	feed ratio H_2/CO	gas flow[1] cc/min	pres. mmHg	cavity length, cm	mode[4]	power[3] watts	resi-dence[2] time,sec	% volume CH_4	IR curve number	Remarks
30714	4/1	83	40	13.8	TE*112	486	1.3	1.30	9	
30715	4/1	83	40	"	"	800	1.3	.87	9	dry ice trap
31301	1/1	83	10	"	"	320	0.33	1.08	19	
31302	1/1	83	10	"	"	610	0.3	0.2	19	
31303	1/1	83	2	"	"	370	.07	0.2	19	
31304	1/1	83	20	"	"	930	.65	0.2	19	
31305	1/1	83	20	"	"	750	.65	0.2	20	
31306	1/1	115	20	"	"	770	0.5	0.15	20	
31307	1/1	83	25	"	"	450	0.8	0.15	20	
31308	1/1	83	35	"	"	350	1.1	0.2	20	
31309	1/1	83	45	"	"	350	1.5	0.2	21	
31310	1/1	83	45	"	"	460	1.5	0.2	21	
31401	1/1	83	10	"	"	847	.33	- -	22	
31402	1/1	83	10	"	"	576	.33	- -	22	
31403	1/1	83	25	"	"	597	.83	- -	22	
31404	1/1	83	2	"	"	437	.07	- -	22	

Table 1. Experimental Data (continued)

run number	feed ratio H_2/CO	gas flow[1] cc/min	pres. mmHg	cavity length, cm	mode[4]	power[3] watts	resi-dence[2] time,sec	% volume CH_4	IR curve number	Remarks
31405	1/1	83	2	13.8	TE*112	634	.07	- -	23	
31406	1/1	83	2	"	"	390	.07	- -	23	
31407	1/1	83	10	"	"	365	.33	- -	23	
31408	1/1	83	10	"	"	600	.33	- -	23	
31409	1/1	83	20	"	"	760	.65	- -	23	
31410	1/1	83	20	"	"	800	.65	- -	23	
31411	1/1	83	35	"	"	355	1.1	- -	23	
31901	4/1	83	15	"	"	550	.50	.22	26	IR mirrors partially covered with $CaSO_4$ dust, concentrations of all materials reduced
31902	4/1	83	15	"	"	565	.50	.44	26	
31903	4/1	83	15	"	"	390	.50	.23	26	
31904	4/1	83	15	"	"	655	.50	.23	26	
31905	4/1	83	25	"	"	380	.80	.34	27	
31906	4/1	83	25	"	"	530	.80	.34	27	
31907	4/1	83	25	"	"	295	.80	.22	27	
31908	4/1	83	2	"	"	700	.07	1.08	28	

Table 1. Experimental Data (continued)

run number	feed ratio H_2/CO	gas flow[1] cc/min	pres. mmHg	cavity length, cm	mode[4]	power[3] watts	resi-dence[2] time, sec	% volume CH_4	IR curve number	Remarks
31909	4/1	83	2	13.8	TE*112	540	.07	1.08	28	
31910	4/1	83	2	"	"	270	.07	0	28	
31911	4/1	83	2	"	"	420	.07	0	28	
31912	4/1	83	2	"	"	590	.07	1.08	28	

Notes:

1. Gas flow at rotameter conditions of 5 psig and 70°F.
2. Residence time based on system pressure and temperature at reactor outlet.
3. Total power absorbed in cavity.
4. Type of mode is dicussed in Part II.

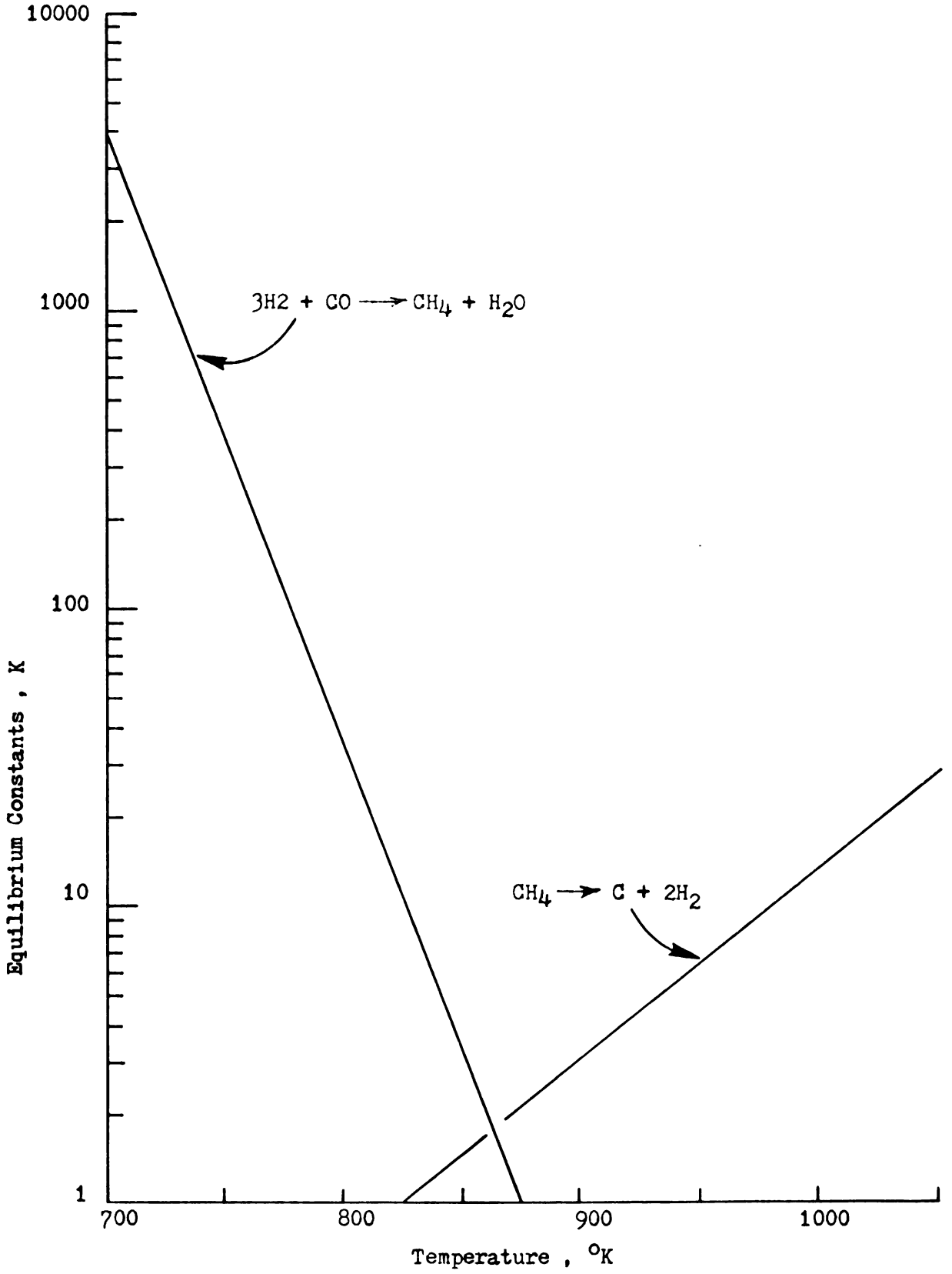

Figure 4. Equilibrium constants for H_2-CO-CH_4 system

H_2 - CO system was used to explain this phenomena. It can be seen that above 850°K any methane formed would be thermally decomposed to carbon. During these runs hot spots were observed in the plasma at the walls, and once the quartz tube started to melt which would indicate temperatures above 1500°K, it was the general conclusion that the reddish electric discharge was too hot a plasma to produce methane.

After these first runs the electrical system was modified by varying the sliding short position on the power divider which reduced the power absorbed in the cavity. Also in order to provide additional cooling a forced air circulation system was installed in the cavity. It was felt that longer residence times would be required in the colder plasma so new rotameters were installed. Coupled with these modifications was the need to change the cavity length to keep the resonant frequency constant. The cavity length was increased to 13.8 cm and this corresponded to the TE*112 hybrid mode (discussed fully in Part II). Since during our initial runs (13001-20104) no trouble was experienced in the generation of the plasma the feed mixture was changed to 4:1 hydrogen to carbon monoxide (by volume). This better reflected the stoichometry of the methanation reaction. After these mechanical modifications the power could be varied from 100-800 watts and the flow between 5-110 cc/min at the rotameter pressure and temperature.

The next experiments (runs 30101-30113) were successful in that methane was produced and identified by the IR bands at 2980 cm^{-1} and 1300 cm^{-1} as shown in IR spectra number 2 and 5. Comparison with IR spectra 3 and 4 also confirms the presence of methane when the plasma was generated. This is the first reported production of methane in a microwave plasma using a continuous flowing H_2 - CO feed. No attempts

were made to maximize the amount of methane in these runs, however methane was observed with flow rates from 75-100 cc/min, residence times of .25 - 1.1 sec, and power levels of 200-300 watts. The plasma consisted of two blueish spherical shaped glows in the quartz tube.

It was necessary to determine qualitatively the amount of methane produced in the plasma for each set of conditions. A gas mixture in a ratio of 37:9:1 of H_2 - CO - CH_4 (representing 10% conversion of CO to CH_4 if no other hydrocarbons are formed) by volume was prepared and analyzed on the IR at a variety of pressures commonly used during experimental runs. These are shown in IR curves 16 and 17. The percent by volume of methane in each run was then determined based on the area under the methane IR peak at 2980 cm^{-1} compared to the standard at the corresponding pressure. The percent by volume in runs 30101-30113 varied from 0.1 - 1.5%.

Once methane had been produced with plasma catalysis it was necessary to determine optimum conditions which would maximize the hydrocarbon yield. One important parameter explored was the residence time, which is a function of both rotameter flow rate, and reactor temperature and pressure. By holding the power and pressure constant, and varying the flow it was found the percent methane in the plasma reactor gas discharge went through a maximum. This is shown in Figure 5. A possible explanation to this experimental observation may be that at longer residence times the bulk gas temperature (or electron temperature) are high enough to thermodynamically favor the reverse reaction or other side reactions such as formation of carbon or acetylene. Figure 4 shows the equilibrium constants for the methanation reaction as a function of temperature.

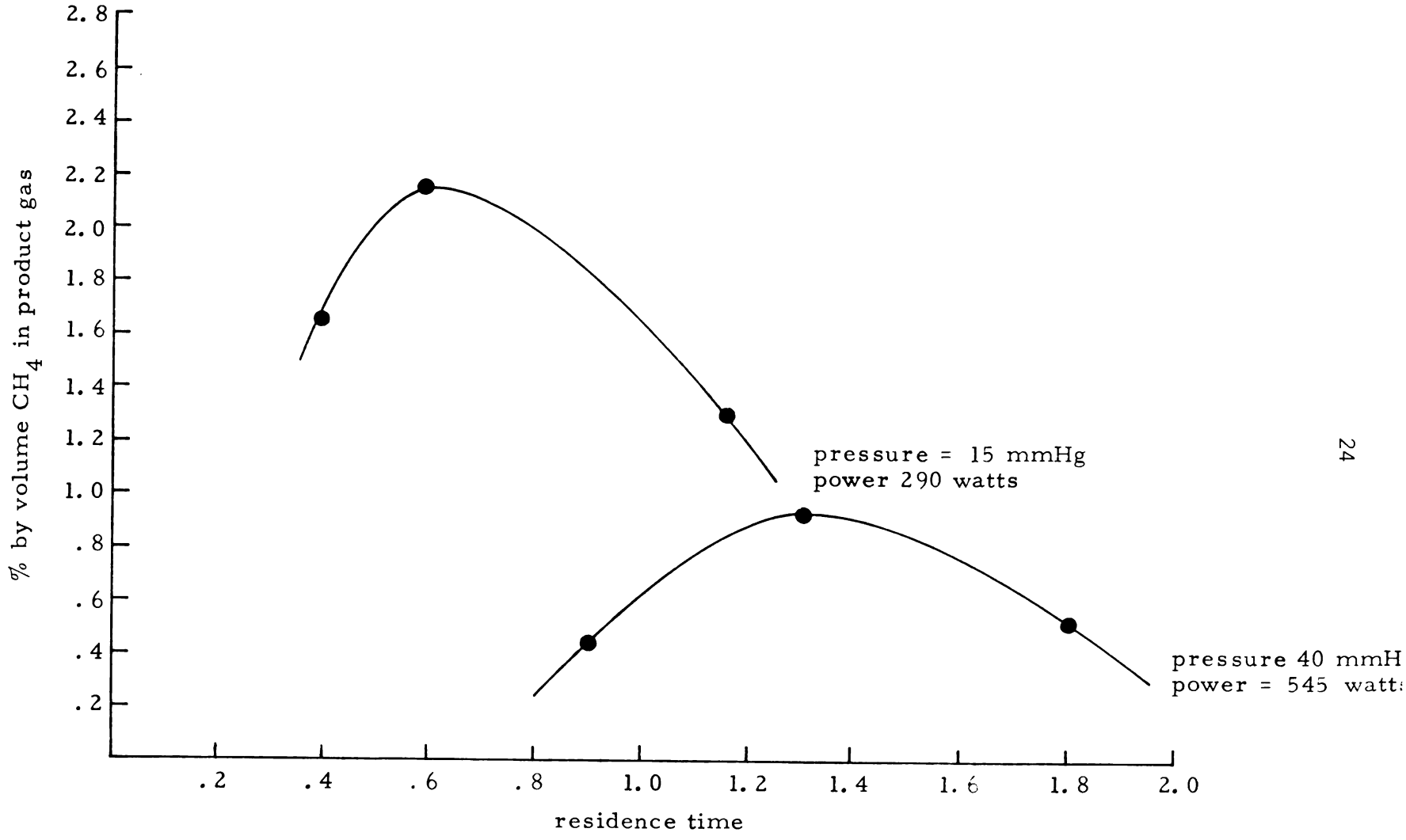

Figure 5 . Methane yield versus residence time

Another variable was the amount of power put into the plasma cavity. As discussed before the plasma characteristics were unfavorable for any hydrocarbon production above 1000 watts. Several runs showed similar results when the pressure and flow were held constant and the power varied. This is shown in Figure 6. Since in order to maintain the plasma it took about 125-175 watts, the optimum power range for methanation lies between 250-650 watts depending on the pressure and flow rate.

The volumetric ratio of hydrogen to carbon monoxide in the feed gas is an important parameter in determining optimum operating conditions. The initial runs (13001-13004) were at a 10:1 ratio and showed no methane, however the power levels were too high and a different cavity length was used which both produced unfavorable conditions. The majority of runs were with a 4:1 H_2 - CO ratio. A special case tested was a 1:1 H_2/CO feed. These experiments resulted in a greatly reduced amount of methane in the product gas stream and required substantially higher power levels to maintain the plasma. IR spectra 20 with runs 31301-31411 shows these experiments. This is consistent with our proposed mechanism in which generation of the hydrogen radical would be the rate controlling step (discussed in Part II). Higher power levels were required since the ionization potential of the CO molecule is much greater than that of hydrogen, and consequently this feed ratio will favor a hotter plasma which is unsuitable for the methanation step.

The effect of pressure on the yield of methane is a very significant factor in establishing the operability and feasibility of the methanation reaction. From the experimental data, the highest yield

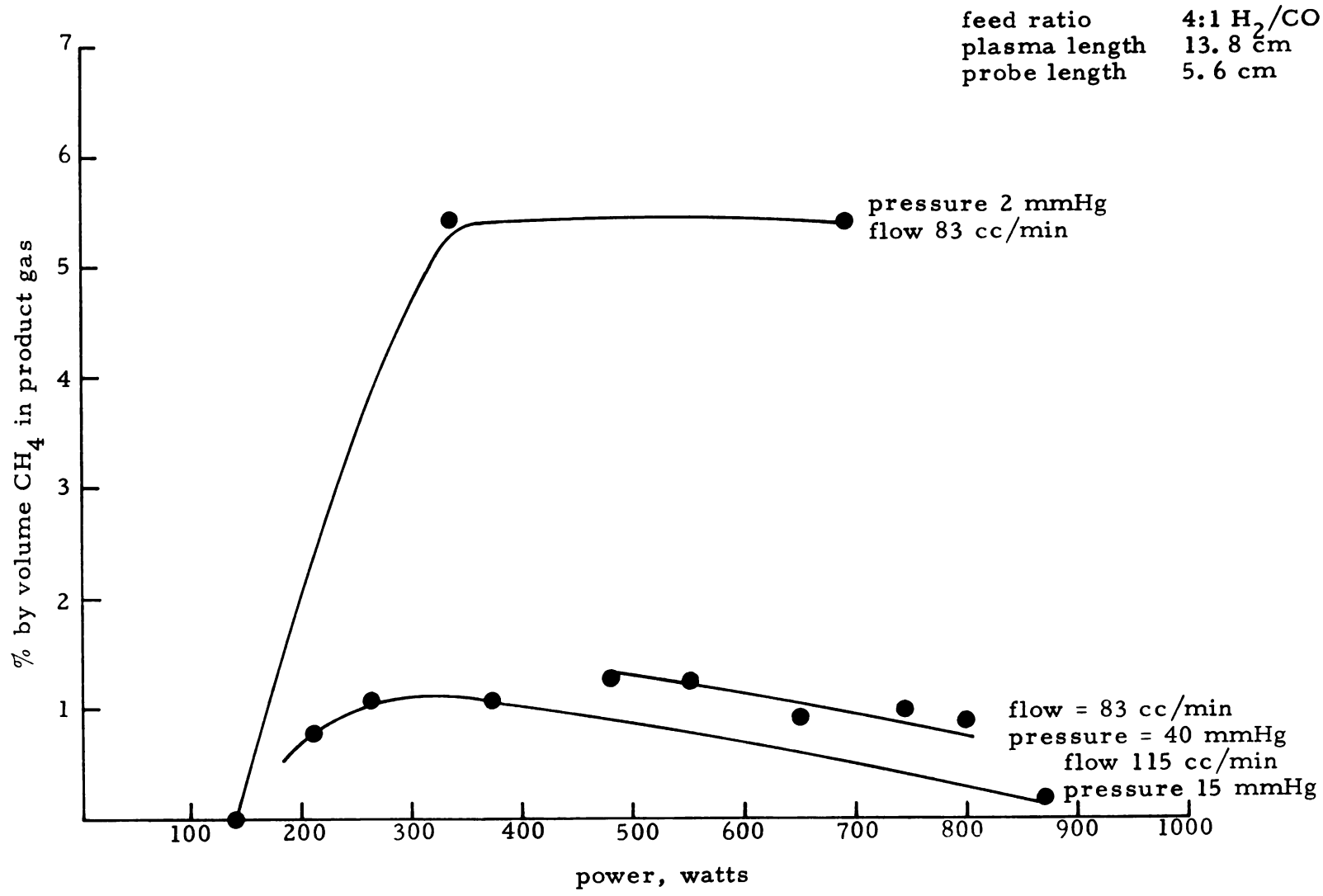

Figure 6 . Methane yield versus power

of methane was 5.4% by volume at 2 mm Hg. This corresponds to approximately 25% conversion of the CO in the flowing feed gas. Bell's[12,13] work showed that at lower pressures the value of K_1, the rate constant for generation of the hydrogen radical, is higher and hence greater chemical reactivity (Figure 8). Our results would seem to indicate this also, however due to different types of electrical discharges and resonant frequencies used this has yet to be fully substantiated. Since the main problem encountered in substaining higher pressures was the plasma becoming too hot above 50 mm Hg, further modifications in the cooling system or establishment of a colder type plasma at higher pressure will be of high priority.

One other hydrocarbon identified in the product gas by mass spectrophotometry was acetylene. Epple and Apt[7] reported this same biproduct in their static system. Because of the very poor sensitivity and broad band acetylene has in the infrared region, it was not possible to determine qualitatively the amount in each run. IR spectra 24, of a 1:1 mixture of methane-acetylene shows this very broad band at 3200-3300 cm^{-1}. Comparing this with the experimental runs recorded on the IR, the amount of acetylene in the product gas would in all cases by much less than the amount of methane.

Further research conducted during the writing of this paper has shown acetylene produced exclusively with a 4:1 H_2 - CO feed using the TE011 mode. The conversion of CO to CH≡CH based on a methane free product was 15% at 15 mmHg and 0.4 sec. residence time.

SUMMARY

This research effort, of the Department of Chemical Engineering and the Department of Electrical Engineering and Systems Sciences, reports the first production of methane in a microwave plasma using a flowing hydrogen-carbon monoxide system. The highest yield found was 5.4% by volume methane in the product gas (corresponding to 25% conversion of CO). Residence times below 2 seconds were found to be most satisfactory and enhance the overall economics of the project. Power levels between 250-650 watts were found to give the highest yields of methane. Pressures were tested between 2-50 mm Hg with the highest conversions obtained at the lower pressures. Acetylene was identified as a biproduct, and a proposed mechanism for the methanation reaction including this side reaction was developed. Significant advancements in the area of high pressure - cold plasma technology allowed hydrocarbon production for the flowing gas mixture.

REFERENCES

1. Venugopalon, M., Reactions Under Plamsa Conditions, Vol. I (Wiley 1968).

2. McTaggart, F. K., Plasma Chemistry in Electrical Discharges, Elsevier, New York (1967).

3. Baddour, R. F., and Timmins, R. S., The Application of Plasma to Chemical Processing, MIT Press, Cambridge (1967).

4. Blaustein, B. D., Advances in Chemistry Series No. 80, A.C.S, Washington, D.C. (1969).

5. Blaustein, B. D. and Fu, V.C., Chemical Reactions in Electrical Discharges, Adv. Chem. Ser. 80, A.C.S, Washington, D.C. (1969).

6. McTaggart, F. K., Australian J. Chem. 17, 1182 (1964).

7. Epple, R. P. and Apt, C. M., The Formation of Methane from Synthesis Gas by High Frequency Radiation, Gas Operations Research Project PF-27, Am. Gas. Assoc. Inc. (July 1962).

8. Wendt, G., and Evans, G. M., J.A.C.S. 50, 2610 (1928).

9. Lunt, R. W., Proc. Roy. Soc. (London) 108A, 172 (1925).

10. Asmussen, J. and Fredericks, R. M., Appl. Phys. Letters, 19, 508 (1971).

11. Asmussen, J., Fredericks, R. M. and Hatch, A. J., Behavior of a Bounded Plasma Inside a Microwave Cavity at High and Low Pressures, submitted to J. Applied Physics in September 1972.

12. Bell, A. T., Ind. Eng. Chem. Fund., Vol. II (1972).

13. Bell, A. T., Chem. Eng. Pro. Symp., Ser. No. 112, Vol. 67, (1972).

14. Asmussen, J., Hawley, M. C., and Wilkinson, B. W., Synthetic Natural Gas from Plasma Catalysted Chemical Reactions, Michigan State Research Proposal (1972).

PART II - THE MICROWAVE PLASMA AS CATALYST FOR THE METHANATION REACTION

DESCRIPTION OF PLASMA CHARACTERISTICS AND PARAMETERS

In the conventional methanation reaction of H_2 - CO a nickel catalyst is employed. It is the purpose of this research to utilize a plasma (or electric discharge) as an economically feasible substitute for the solid catalyst. It is important to emphasize that only the energy for maintaining the plasma for catalysis will be put into the system with the microwave source. The minimum energy required to maintain a microwave plasma has been estimated to be 150 watts. Just as the reaction rate is a function of such parameters as porosity and pore size of the solid catalyst pellet, the plasma parameters such as electron density, electron temperature, and electric field strength determine the overall kinetics and reaction rate. Electric discharges are classified into two types, an "E-discharge" and "H-discharge." The methanation within the plasma reactor is of the E-type discharge which is characterized by low bulk gas temperatures and high electron temperatures (2000 - 10,000°K). A H-type discharge in a gaseous system possesses equal electron, ion, and neutral particle temperatures of up to 10,000°K.

An important parameter in the plasma system is the electron density which is nonuniform both axially and radially in the quartz tube plasma reactor. This nonuniformity of the electric discharge results in a plasma reactor with only zones of high reaction efficiency. In our work usually two or three zones were visible for the methanation using H_2 and

CO. Also radial zones, or rings, leave open the possibility of bypassing thus causing low chemical and electrical conversion efficiencies (Figure 7). Mathematically the electron density, or concentration can be expressed as

$$u_f \frac{\partial N_e}{\partial Z} + \frac{D}{r^2} \frac{\partial^2 (r^2 N_e)}{\partial r^2} + D \frac{\partial^2 N_e}{\partial Z^2} = R_{ionization} = N_e \nu_{ionization}$$

where D is the ambipolar diffusion coefficient which can be expressed as a function of the electron energy, kT_e, and a mobility term μ_e. The rate of ionization, R, is proportional to the electron density and is conventionally defined as $N_e \nu_{ion}$, where ν_{ion} is the ionization frequency.

In characterizing a plasma the concept of temperature is difficult to define. This is because the kinetic theory relates temperature to the kinetic energy of the gas molecules. However, the electrons will have very high kinetic energies due to their relatively low masses and very high velocities which gives an "electron temperature" that is much larger than the "kinetic temperature." Thus defining rate constants can be made possible by use of an "equivalent temperature" defined by Epple and Apt[8] as the equilibrium temperature to which the system would have to be brought in order to attain the composition observed on chemical analysis of the constituents.

In an electric discharge or plasma it has been found that the suitable parameter to describe the system is E/p, where E is the electric field strength and p the total pressure. Previous work[3,5] has shown that at higher values of E/p, the average electron energy is larger, thus the chemical reactivity of the system is greater (Figure 8). This occurs since electrons have a larger acceleration at higher values of E and at lower pressures. The smaller number of collisions occurring at low

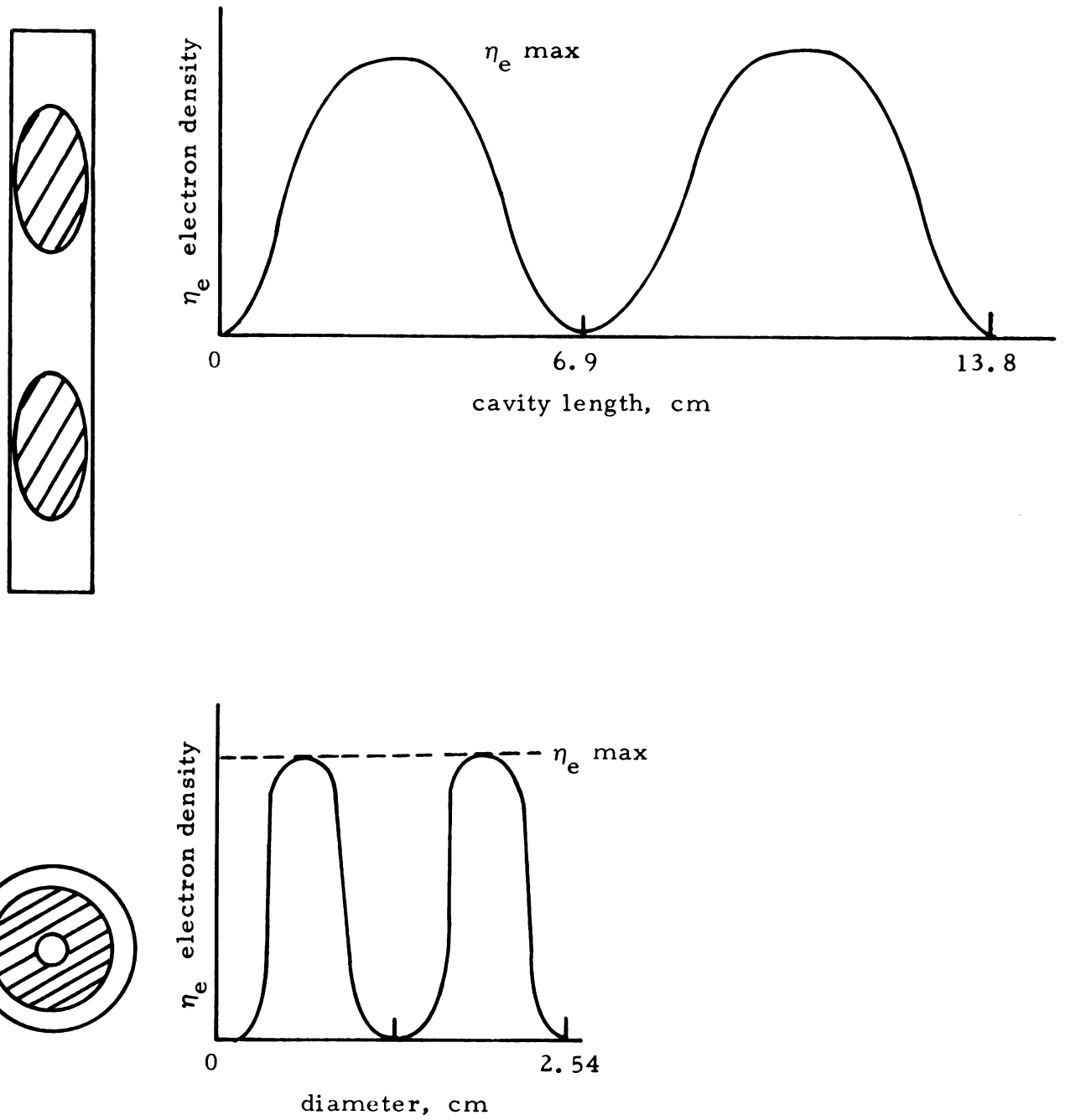

Figure 7 . Electron density as a function of length and radius for the TE^* 112 mode

pressure permit an electron to gain large amounts of energy. It should be noted that all work on this area has been on systems with low electron densities using batch type reactors. The methanation reaction is in a flowing system with electron densities suspected to be much higher than those previously explored.

MICROWAVE PLASMA CHEMISTRY AND PROPOSED REACTION MECHANISM

The microwave plasma source will produce a nonequilibrium plasma with a large number of free radicals at low bulk gas temperatures.[6,7] This is made possible through use of the cold E-type discharge.[6] Besides free radicals ionic species can be generated from interactions between the atomic and molecular hydrogen species, however their effect on the overall reaction rate and kinetics are neglectible. In a steady state discharge the concentration of H_2^+ is governed by the rate of its formation through ionization of molecular hydrogen. Since the plasma is approximately neutral the concentration of H_2^+ is considerably below that of the free electrons. Yamone[1] reported rate constants for generation of H_2^+ two orders of magnitude smaller than the corresponding free radical rate.

For the H_2 - CO - CH_4 - H_2O system in a plasma reactor a multitude of reactions could possibly occur as listed below (eqn 1-11).

Initiation

(1) $H_2O \rightarrow O\cdot + OH\cdot$

(2) $CO + H\cdot \rightarrow CO\,H\cdot$

(3) $CH\cdot + H_2 \rightarrow CH_2\cdot + H\cdot$

(4) $CH_2\cdot + H_2 \rightarrow CH_3\cdot + H\cdot$

Propagation

(5) $CO + OH\cdot \rightarrow CO_2 + H\cdot$

(6) $CH_3\cdot + H_2 \rightarrow CH_4 + H\cdot$

(7) $OH\cdot + H_2 \rightarrow H_2O + H\cdot$

Termination

(8) $CH\bullet + CH\bullet \rightarrow CH \equiv CH$

(9) $CH_2\bullet + CH_2\bullet \rightarrow C_2H_4$

(10) $CH_3\bullet + CH_3\bullet \rightarrow C_2H_6$

(11) $H\bullet + H\bullet \rightarrow H_2$

The reaction mechanism proposed for the methanation step is shown in equations 12-16. Included in this is a heterogenous recombination term due to hydrogen radicals diffusing to the wall and recombining. This mechanism is purely speculative for the methanation in a plasma, however does incorporate the basic [CH•] intermediate which would be required to produce CH_4 and CH ≡ CH found in our experimental work.

(12) $e + H_2 \xrightarrow{k_1} 2H\bullet$

(13) $CO + H_2 + H\bullet \xrightarrow{k_2} CH\bullet + H_2O$

(14) $CH\bullet + 2H_2 \xrightarrow{k_3} CH_4 + H\bullet$

(15) $2CH\bullet \xrightarrow{k_4} CH \equiv CH$

(16) $2H\bullet \xrightarrow{k_w} H_2$

At equilibrium the rate of formation of CH• and H• can be assumed to be equal to zero ($d(CH\bullet)/dt = 0$). Additionally the wall recombination rate constant can be assumed to be small compared to k_3 and k_4. Based on these assumptions the rate of formation of methane and acetylene are shown in equations 17 and 18.

(17) $r_{CH_4} = k_3[CH\bullet][H_2]^2 = 1.41\ k_3\ [H_2]^{5/2}(k_1/k_4)^{1/2}[N_e]^{1/2}$

(18) $r_{CH \equiv CH} = k_4\ [CH\bullet]^2 = 2\ k_1\ [N_e][H_2]$

It should be noted that for this proposed mechanism both the rates are independent of the carbon monoxide concentration. This is due to the fact that the rate controlling step is the formation of the hydrogen radical governed by k_1. Experimental evidence has shown the ratio of the rate of formation of methane to acetylene is on the order of .01 - 1 and using an electron density of 10^{10} cm^{-3} the values of k_3 and k_4 can be estimated to be between 100 - 1000 $(cm^3)^2/mole^2$ sec. This compares favorably with experimentally determined rate constants for other free radical reactions.[8]

Generation of the CH• and H• radical in the plasma reactor will be the rate controlling steps since both of these are highly reactive intermediates. The dissociation rate constant k_1 is conventionally defined in an electric discharge (Equation 19) from the

$$(19) \quad k_1 = (8/\pi M_e)^{1/2}(kT_E)^{3/2} \int_0^\infty \varepsilon \, \sigma \exp(-\varepsilon/kT_E) d\varepsilon$$

M_e = mass of electron

kT_E = electron energy

ε = dissociation energy

σ = dissociation cross section

Maxwell-Boltzman distribution of electron energies. Khare and Moiseiwitsch[2] theoretically determined values for the dissociation cross section for the excitation of ground state molecular hydrogen to the replusive state. In their work they considered this the only process contributing to the dissociation and their calculated values were in good agreement with previous experimental findings by Poole.[4] Bell[3,5] has determined k_1 for the excitation of hydrogen as a function of electron

temperature (or E/p the ratio of electric field strength to gas pressure). This is shown in Figure 8.

The formation of the CH• radical can be visualized as a bimolecular insertion of H• to the CO molecule, forming a pseudo intermediate CO H• which combines with a hydrogen molecule to give the CH• intermediate and a water molecule.

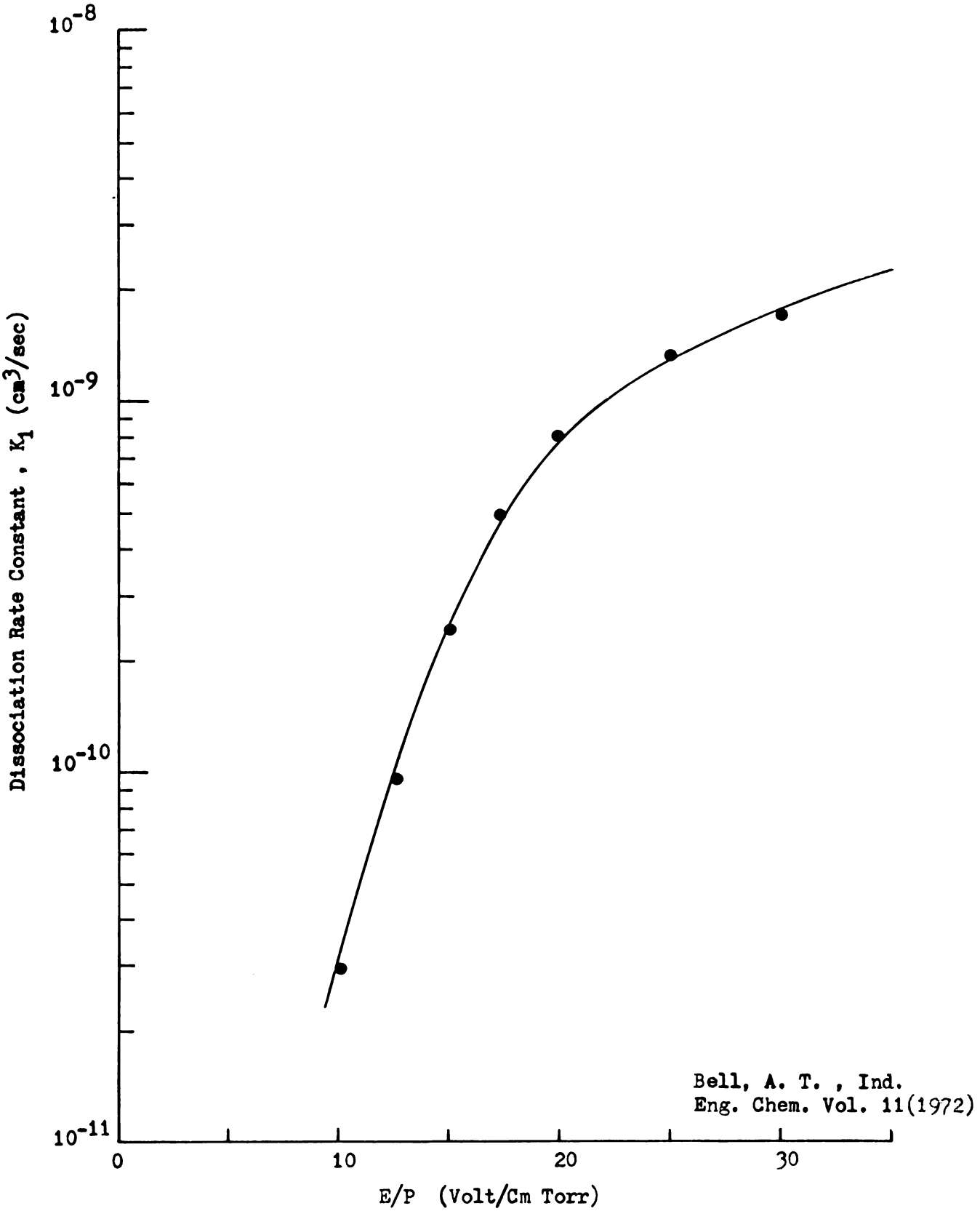

Figure 8 . Dissociation rate constant K_1 versus electric field strength divided by pressure .

MICROWAVE PLASMA REACTOR AND RF SYSTEM

The microwave plasma cavity is shown in Figures 2,9,10. The reactant gases pass through the plasma created in the quartz tube while pressures in the system can be varied from 2-100 mm Hg. Cooling is provided by water coils on the cavity and forced air circulation through the cavity. A probe coupling allows the rf energy to be introduced into the cavity and produce the plasma. This probe length can be adjusted which changes the effective electrical field strength producing variations in reaction rates and electron density. Radial and axial measurements of the electrical field strength is accomplished through small ports in the cavity. The adjustable cavity length serves to retune the plasma as power, pressure, and probe length are varied. Adjustment of the cavity length keeps the plasma resonance equal to the excitation frequency.

The left-hand group of curves in Figure 11 demonstrates the behavior of the plasma cavity when the excitation frequency and the cavity size are fixed. The stable operating points, a,b, show that as the incident power is increased the plasma density increases relatively little. The plasma cavity system adjusts itself to a stable operating point, a, which is determined primarily by the plasma cavity resonant frequency, (i.e., cavity dimensions and excitation frequency). When the incident power is greatly increased the operating point moves to point b and the cavity becomes more detunned. That is, only a small

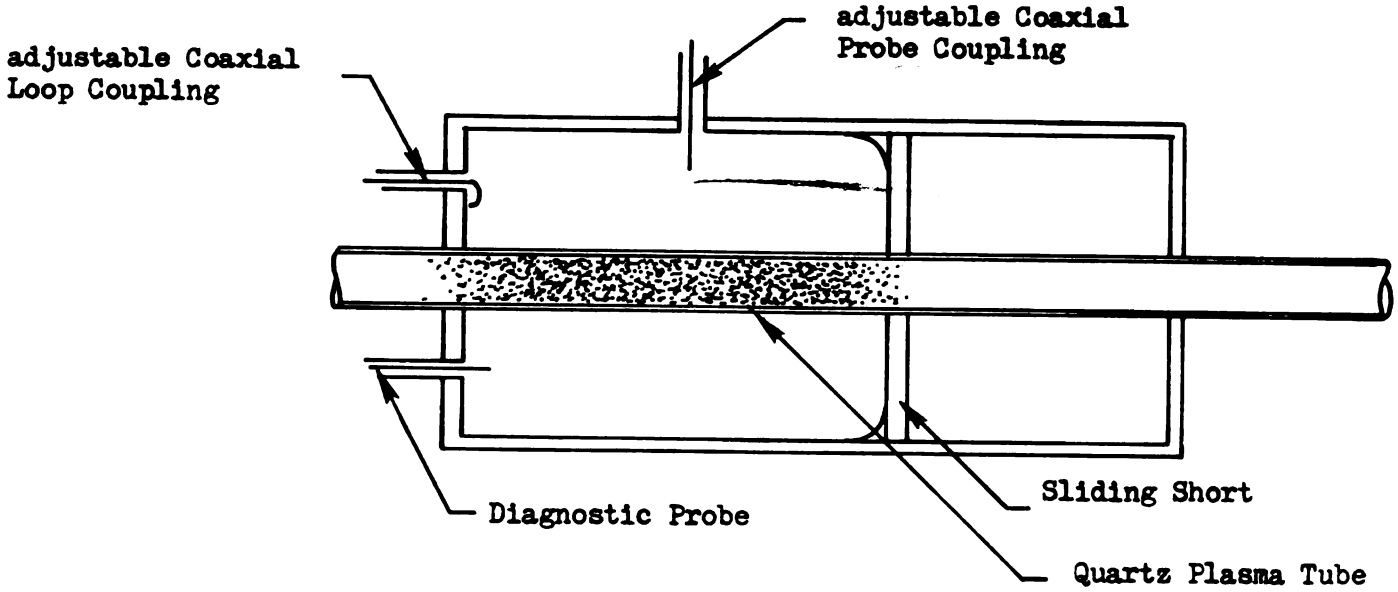

CROSS SECTION OF PLASMA REACTOR

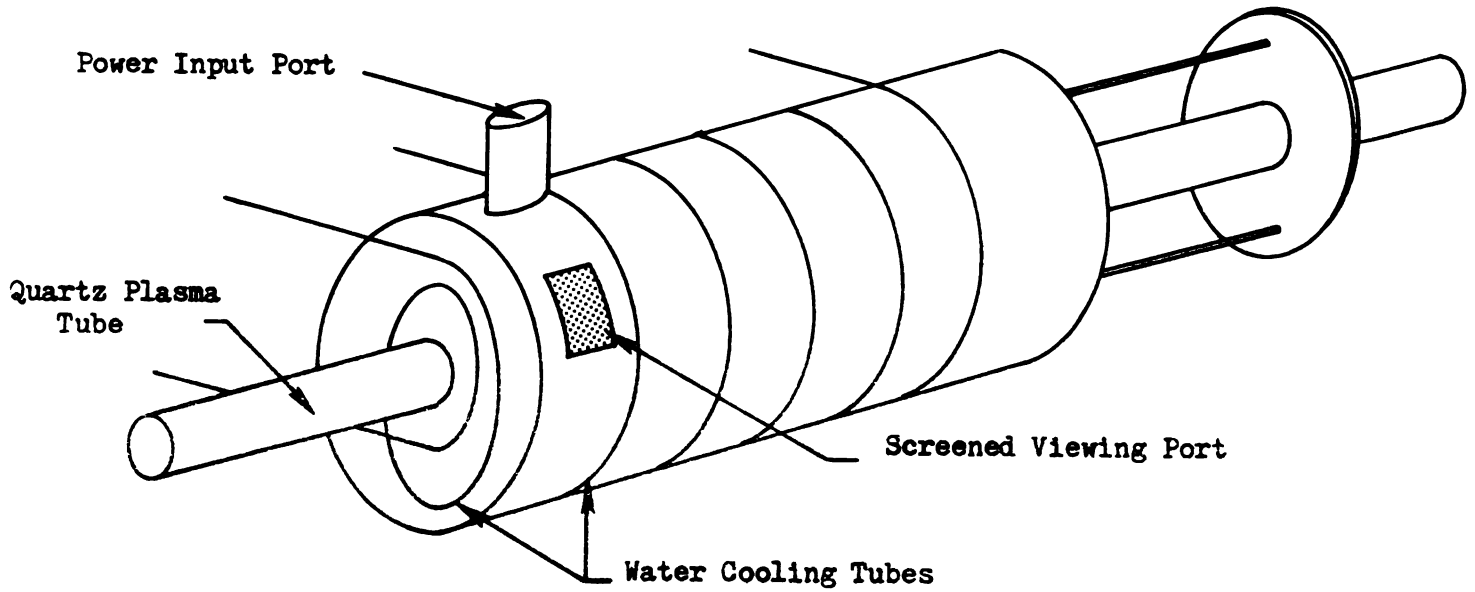

ISOMETRIC DRAWING

Figure 9. Cylindrical Plasma Reactor

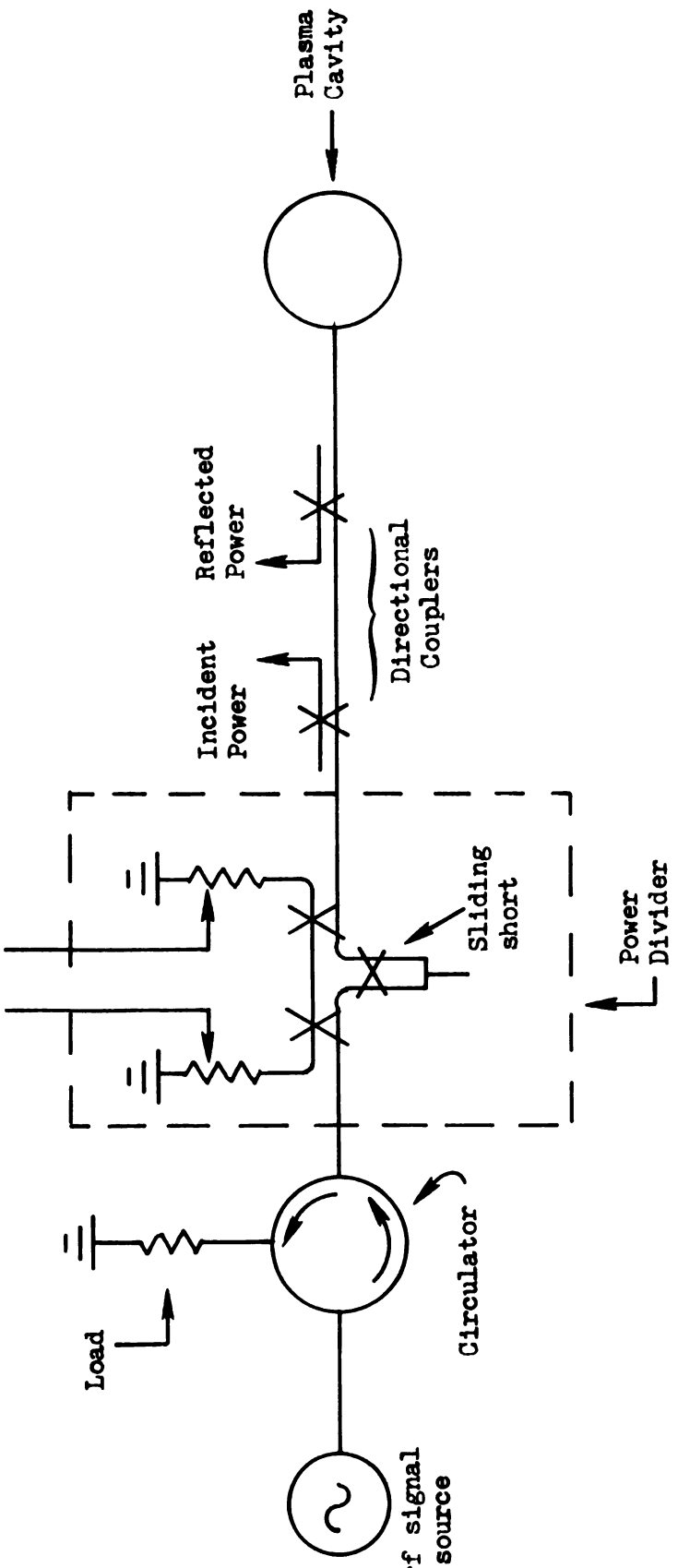

Figure 10 . The rf system

fraction of the additional incident power is absorbed into the plasma and the excess power is reflected from the cavity. Thus the detunning of the system by the presence of the plasma does not allow a significant fraction of the additional incident power into the cavity. Even the addition of impedance matching devices between the cavity and the input transmission line only slightly improves the cavity system performance[9]. This small change in density for a large change in incident power is a fundamental problem when attempting to produce a variable, high density plasma inside a microwave cavity.

One proposed solution to this problem is to continuously vary the excitation frequency while the rf plasma is sustained. Halverson and Hatch[9] have shown that by increasing the excitation frequency while holding the incident power constant the density of a rf plasma inside the cavity can be increased seven times. However, this frequency tunning generally requires an expensive rf source and is a tedious process.

An alternative solution is to continuously vary the cavity dimensions. Fredericks and Asmussen[10] have shown that cylindrical, variable length cavities can be tuned to allow the variation of the plasma density from less than one critical density to over 10 critical densities at low pressures. The performance of these cavities can be qualitatively understood by examining the graphical model as a function of cavity length L. By holding in incident power constant at P_{in3} and increasing the cavity length from L_1 to L_2 to L_3 the power absorbed curve shifts to higher densities as shown in Figure 11. For length L_1 the empty cavity resonant frequency equals the excitation frequency. When the incident power is increased to P_{in3} breakdown occurs inside the cavity and a microwave plasma is sustained at the stable operating point b.

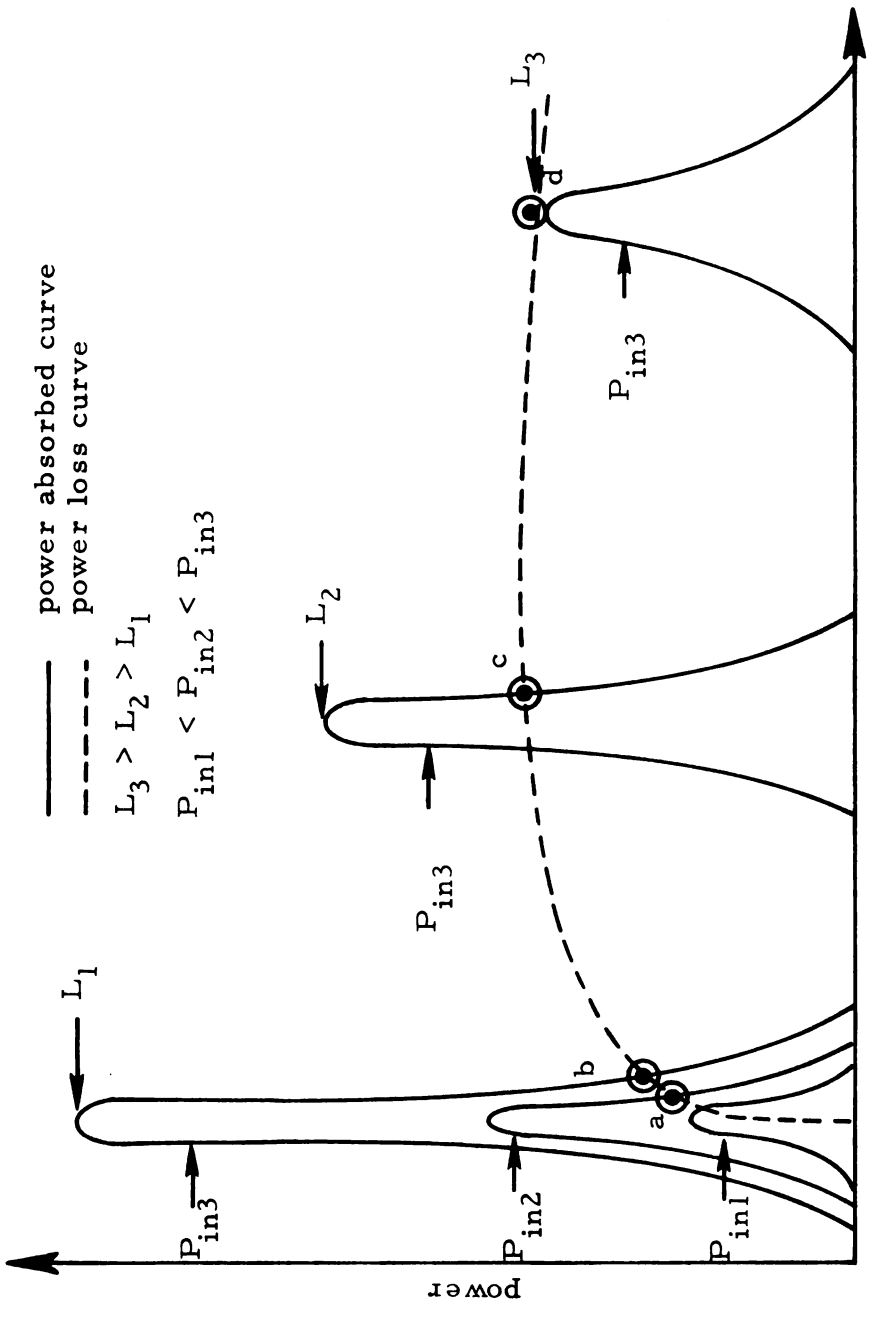

Figure 11. Behavior of the plasma cavity when the excitation frequency is constant.

By continuously increasing the cavity length the cavity becomes progressively better tuned and the absorbed power and hence density increase tracing out the power loss curve bcd. Finally, a cavity length, L_3, is reached at point d where the intersection between the power absorbed curve and the loss line is only marginally stable. For any length larger than L_3 the plasma is abruptly extinguished and the plasma cavity system drops out of resonance. In order to reignite the plasma the cavity length must be reduced to approximately L_1.

The curves of Figure 11 have been plotted for a constant pressure and fixed cavity input coupling. Altering the pressure will change both the power loss and power absorbed curves, while altering the input coupling will modify the power absorbed curves. It is important to remember that there can exist pressures when the slope of the power loss curve is always greater than the power absorbed curves. Then all intersections between these two curves will be stable operating points. Note also that increasing the plasma density decreases the coupling of energy to the plasma[11], i.e., given the incident power P_{in3}, the height of the power absorbed curves decreases as the density increases.

The transfer of energy from the microwave rf source of the gas molecules is brought about by electrons undergoing collisions with the gas molecules. Electrons gain and accumulate thermal energy until a sizeable fraction of the total collisions they undergo with the gas molecules change from elastic to inelastic. When the electron undergoes an inelastic collision it imparts a large fraction of its total energy which results in the excitation or ionization of the gas.

In order to describe the microwave plasma mathematically Maxwell's equations are solved for the different fields. Maxwell's equation in

the electromagnetic theory (EM) relates the electric ($\vec{E}$) and magnetic ($\vec{B}$) fields to the current density ($\vec{J}$) and charge density (ρ) which produce these fields. Except in the case of a static system, $\vec{E}$, $\vec{B}$, ρ, and $\vec{J}$ are time varying quantities. In the mathematical development it is more convenient to define $\vec{D}$ and $\vec{B}$ in terms of $\vec{E}$ and $\vec{H}$.

(20) $\vec{D} = \varepsilon_o \varepsilon_r \vec{E}$

(21) $\vec{B} = \mu_o \mu_r \vec{H}$

where ε_o = permittivity of free space
μ_o = permeability of free space
ε_r = relative dielectric constant
μ_r = relative permeability

For a plasma medium with time harmonic fields (varying as $e^{i\omega\tau}$) we can write Maxwell's equations 22-25.

(22) $\nabla \cdot \vec{E} = 0, \rho = 0$

(23) $\nabla \cdot \vec{H} = 0$

(24) $\nabla \times \vec{E} = - j\omega\mu_o \vec{H}$

(25) $\nabla \times \vec{H} = j\omega\varepsilon_o \vec{E} + \vec{J}$

If equation (25) is expanded for the case of a weakly ionized plasma, then the contribution $\vec{J}$ is mainly from the motion of the electrons (26).

(26) $\vec{J} = - n_e e\vec{V}$

where n_e = electron density cm^{-3}
e = charge on electron
$\vec{V}$ = macroscopic velocity of electrons

From Boltzmann's equation in plasma theory $\vec{V}$ can be related to the electric field strength (equation 27) and rewriting equation (25) in

(27) $\overline{V} = -e\vec{E}/m(j\omega + \nu)$

where m = mass of electron
ω = operating frequency
ν = collison frequency of electrons

terms of this gives the following (equation 28)

$$(28)\quad \nabla \times \vec{H} = j\omega\varepsilon_o \vec{E} + \frac{\eta_e^2 (\nu - j\omega)\ \vec{E}}{m(\nu^2 + \omega^2)}$$

$$\nabla \times H = j\omega\varepsilon_o E \left(1 - \frac{\omega_p^2}{\nu^2 + \omega^2} - j \frac{\nu}{\omega} \frac{\omega_p^2}{(\nu^2 + \omega^2)} \right)$$

where $\omega_p = (\eta_e e^2/m\varepsilon_o)^{1/2}$ = plasma electron frequency.

Instead of defining a complex conductivity for the plasma we can establish an equivalent relative dielectric constant, ε_r, which

$$(29)\quad \varepsilon_r = (\varepsilon_r - j\varepsilon_i) = 1 - \frac{\omega_p^2}{\nu^2 + \omega^2} - j \frac{\nu}{\omega} \frac{\omega_p^2}{(\nu^2 + \omega^2)}$$

where $\varepsilon_r = 1 - \dfrac{\omega_{pe}^2}{\nu^2 + \omega^2}$ and $\varepsilon_i = \dfrac{\nu}{\omega} \dfrac{\omega_{pe}^2}{\nu^2 + \omega^2}$

is characterized by specifying the density, i.e., $(\omega_p/\omega)^2$, and ν/ω.

The detailed derivation of the general characteristic equation for the eigenfrequencies has been carried out by others.[12,13] A computer solution for the general characteristic equation for the TE^*_{111} is displayed in Figure 12. For direct comparison with experimental results resonant cavity lengths are calculated instead of the usual resonant frequencies. That is, given a constant resonant frequency equal to the excitation frequency of 2.450 GHz the resonant length of the cavity is plotted as a function of plasma frequency and ν/ω. Due to the presence of the plasma free space boundary at r = a both transverse electric and magnetic modes are required to satisfy the boundary conditions[12,14] Thus resonant modes of this structure cannot, in general, be separated into purely transverse electric (TE) and transverse magnetic (TM) modes, but most modes have both TE and TM parts and are called hybrid modes.[12] Because of the hybrid nature of the cavity

resonances and the introduction of new modes by the plasma the usual cavity mode identification scheme is not applicable. It is convenient to classify the resonant frequencies as such.

1. "Perturbed" cylindrical cavity resonances.

The resonances are the empty cavity electromagnetic resonances which are "perturbed" by the presence of the plasma. Thus the forward and backward traveling waveguide modes associated with these resonances always have a phase velocity greater than the speed of light, i.e., they are fast wave electromognectic modes. This group of resonances can be further divided into two subclasses of modes:

a. TE_{0mp} or TM_{0mp}; $m > 0$.

These resonances are pure TE and TM resonances since they are ϕ independent and thus they are labeled with respect to the TE and TM modes on a circular waveguide. At high plasma densities and for high losses these modes approach the coaxial mode that has the same index as the empty cavity.

b. TE^*_{nmp} or TM^*_{nmp}; $n > 0$, $m > 0$.

These modes are hybrid resonances. They are labeled with respect to the TE or TM modes in an empty circular waveguide into which they degenerate when the plasma density equals zero. As has been used by others[12] the asterisk denotes the hybrid modes. It is useful to note that for high plasma densities and zero losses (i.e., $\nu/\omega = 0$) the TE^*_{nmp} resonance (or TM^*_{nmp} resonance) approaches the TM_{nmp} resonance (or $TE_{n, m+1,p}$ resonance) in a coaxial waveguide with a metallic center conductor. The TE^*_{111} mode shown in Figure 12 belongs to this family of modes. However, for large values of collision frequency (i.e., for a lossy plasma) the resonant frequency increases, decreases, and then

increases again returning to the TE_{111} coaxial cavity resonant frequency. This is shown in Figure 12 for $\nu/\omega = 0.6$ or larger.

The plasma-cavity could be operated in many different cavity resonances simply by adjusting the cavity length and input coupling. For example, the following empty cavity modes have eigenfrequencies equal to 2.450 GHz when the cavity is varied from 6 cm to 20 cm. TE_{111}, TM_{011}, TE_{211}, TE_{011}, TM_{111}, TE_{112}, TM_{012}, TE_{212}, TE_{012}, TM_{112}, TE_{113}, etc. With the proper cavity length and rf coaxial coupling (i.e., loop or probe) the plasma cavity system will sustain a plasma on any of these modes. However, only the TM_{01p}, TE_{011p} modes, where $p = 1,2$, or 3, were studied extensively.

Figure 10 shows the diagram of the external rf system. The rf source used for the plasma generation was a 2.45 GHz magnetron oscillator which delivers 1 kw of continuous wave power. The rf power passes through a circulator and power divider where the sliding short is used to vary power. The power passes through the incident and reflected couplers where the total power incident on the cavity can be calculated (equation 30). The power incident on the cavity is fed into a coaxial

(30) $$\text{total power incident on cavity} = 2.72\ (\text{incident power}) - 1.53\ (\text{reflected power})$$

system, and the probe length couples the power into the different resonant modes of the plasma.

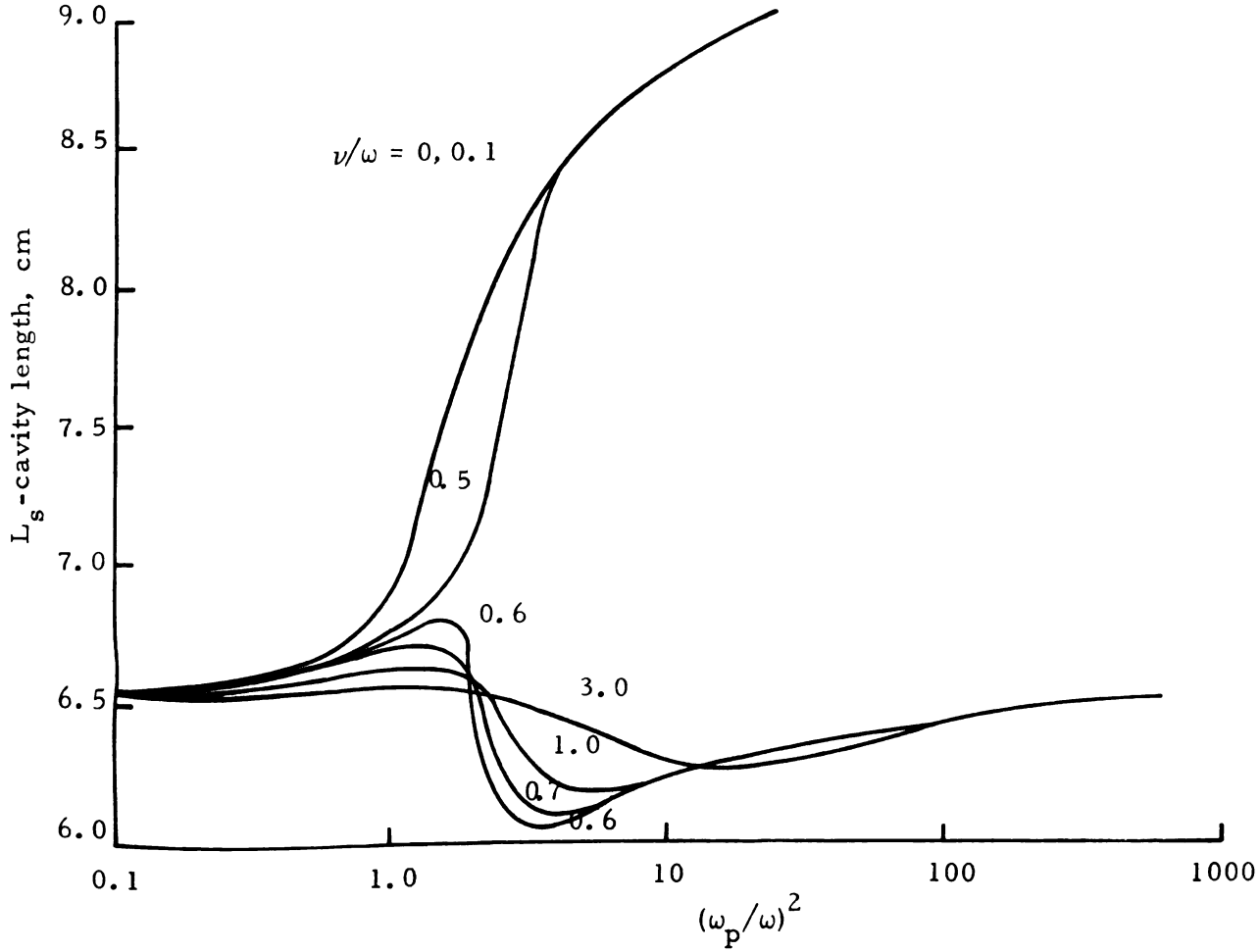

Figure 12. The TE* 111 mode used in experimental work.

REFERENCES

1. Yamane, M. J., Chem. Phys. 49, 4624 (1968).

2. Khare, S. P., Proc. Phys. Soc. 88, 607 (1966).

3. Bell, A. T., Ind. Eng. Chem. Fund. Vol. II (1972).

4. Poole, H. G., Proc. Roy. Soc. Ser. No. I, 415, 424 (1937).

5. Bell, A. T., Chem. Eng. Pro. Symp. Ser. No. 112 Vol. 67, (1972).

6. Babat, G. I., J. Inst. Elect. Engrs. 94, 27 (1947).

7. Asmussen, J., Hawley, M. C., and Wilkinson, B. W., Michigan State Research Proposal (1972).

8. Epple, R. P., and Apt, C. M., The Formation of Methane from Synthesis Gas by High Frequency Radiation, Gas Operations Research Project PF-27, Am. Gas Assoc. (July 1962).

9. Halverson, S. L., and Hatch, A. J., Appl. Phys. Letters, Vol. 14, pp. 79-81, (1969).

10. Fredericks, R. M., and Asmussen, J., J. Appl. Phys., Vol. 42, pp. 3647-9 (1971).

11. Boyen, H. L., Messiaen, A. M., and Vandeplas, P. E., J. Appl. Phys., Vol. 40, pp. 2296-2305 (1969).

12. Agdur, B., and Eneander, B., J. Appl. Phys., Vol. 33, pp. 575-581 (1962).

13. Shohet, J. L., and Moskowitz, C., J. Appl. Phys., Vol. 36, pp. 1756-1759 (1965).

14. Harrington, R. F., Time Harmonic Electromagnetic Fields, New York, McGraw-Hill, pp. 219 (1961).

APPENDIX A

Infrared Spectra for Methanation Reaction

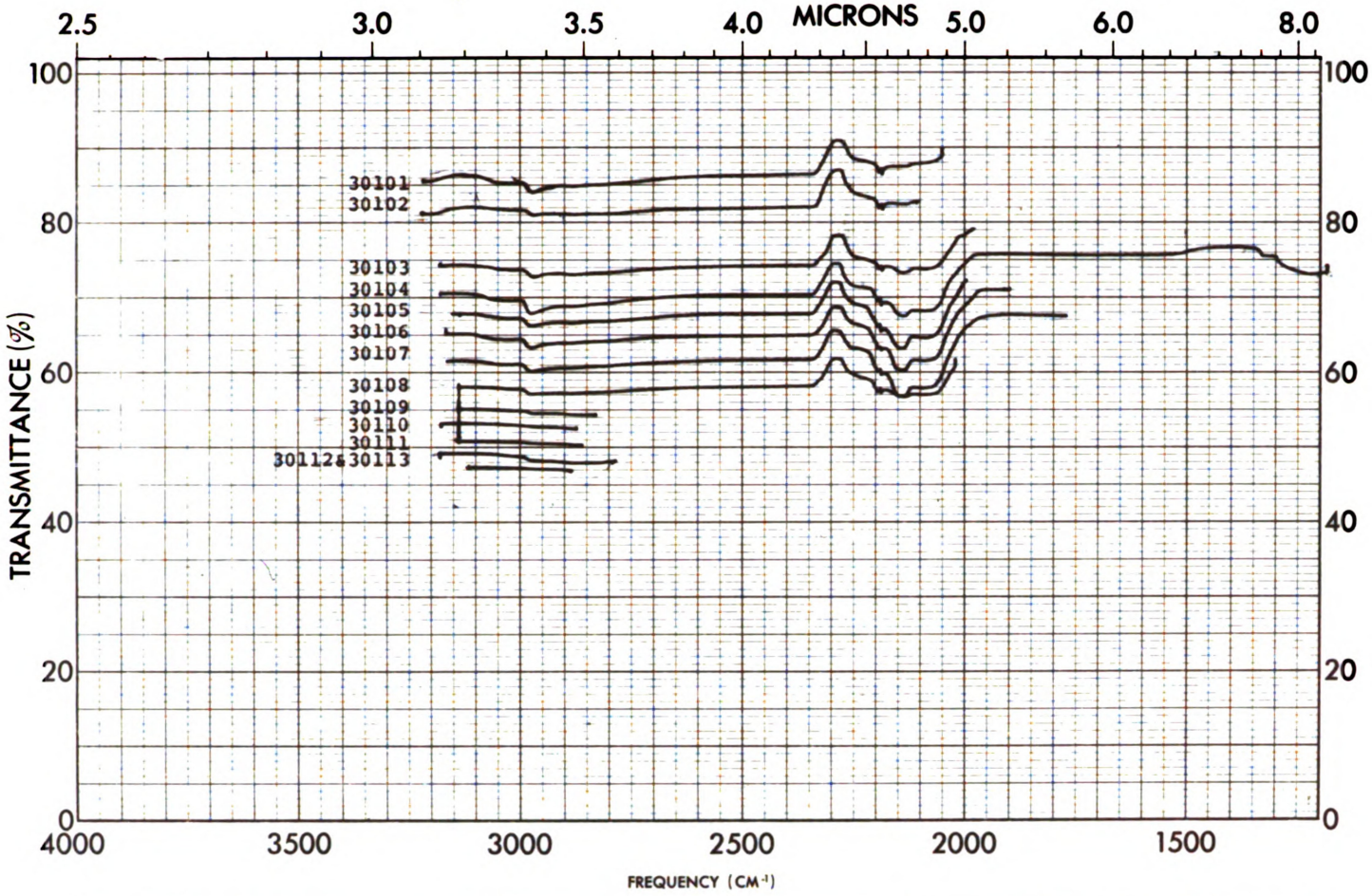

SAMPLE FLOW EXP. 00/4 20%CO	INFARED SPECTRA 2	SCAN SPEED FAST	OPERATOR RLH
		SLIT 10	DATE 3/1/73
ORIGIN		REMARKS	
SOLVENT			

PART NO. 337-1203

PERKIN-ELMER ®

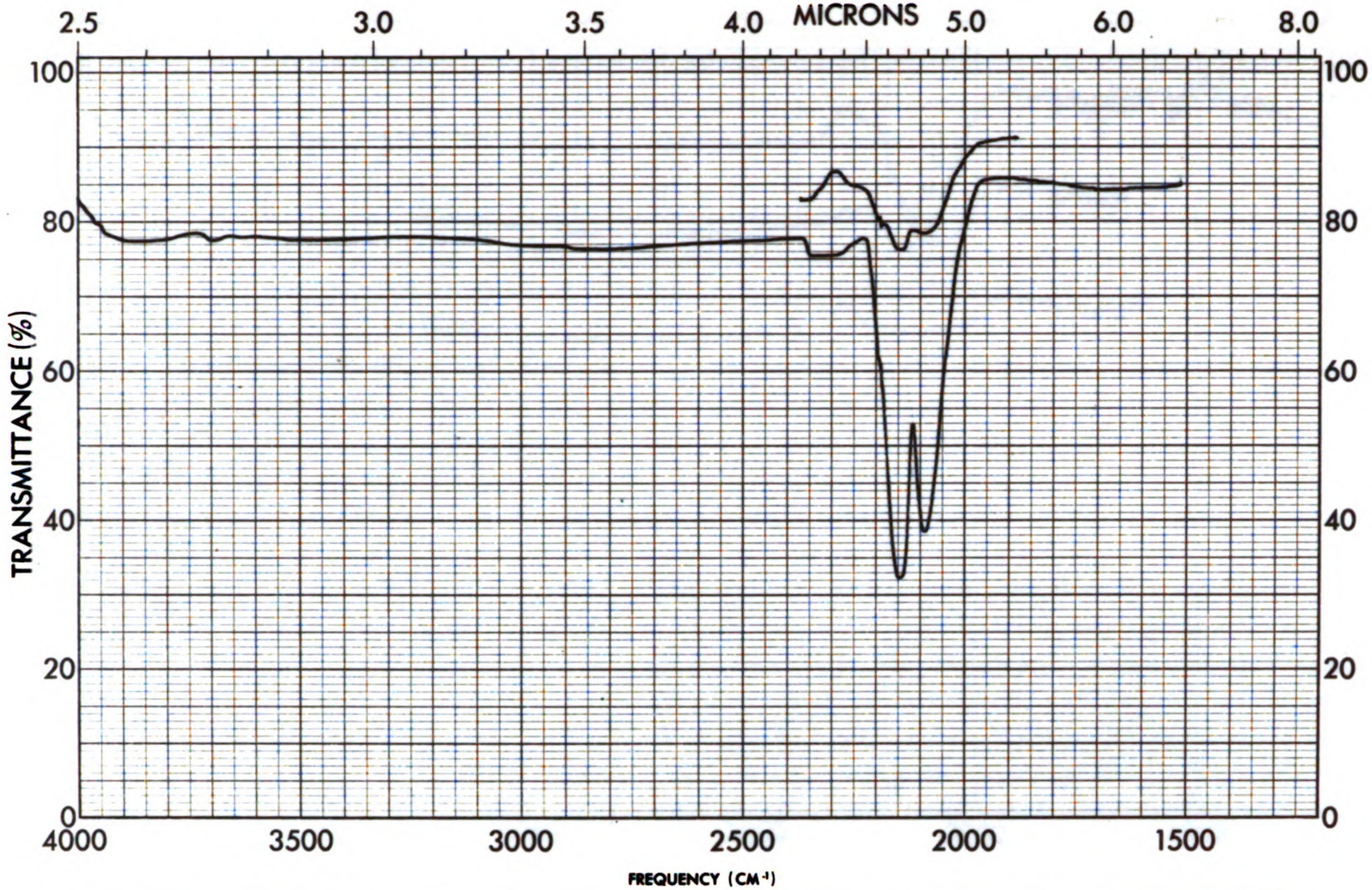

SAMPLE CO/H_2 20% 50 mm Hg & 260 mm Hg ORIGIN 1000 cc/min SOLVENT	INFARED SPECTRA 3	SCAN SPEED FAST SLIT 10 REMARKS	OPERATOR RLH DATE 3-1-73

PART NO. 337-1203

PERKIN-ELMER ®

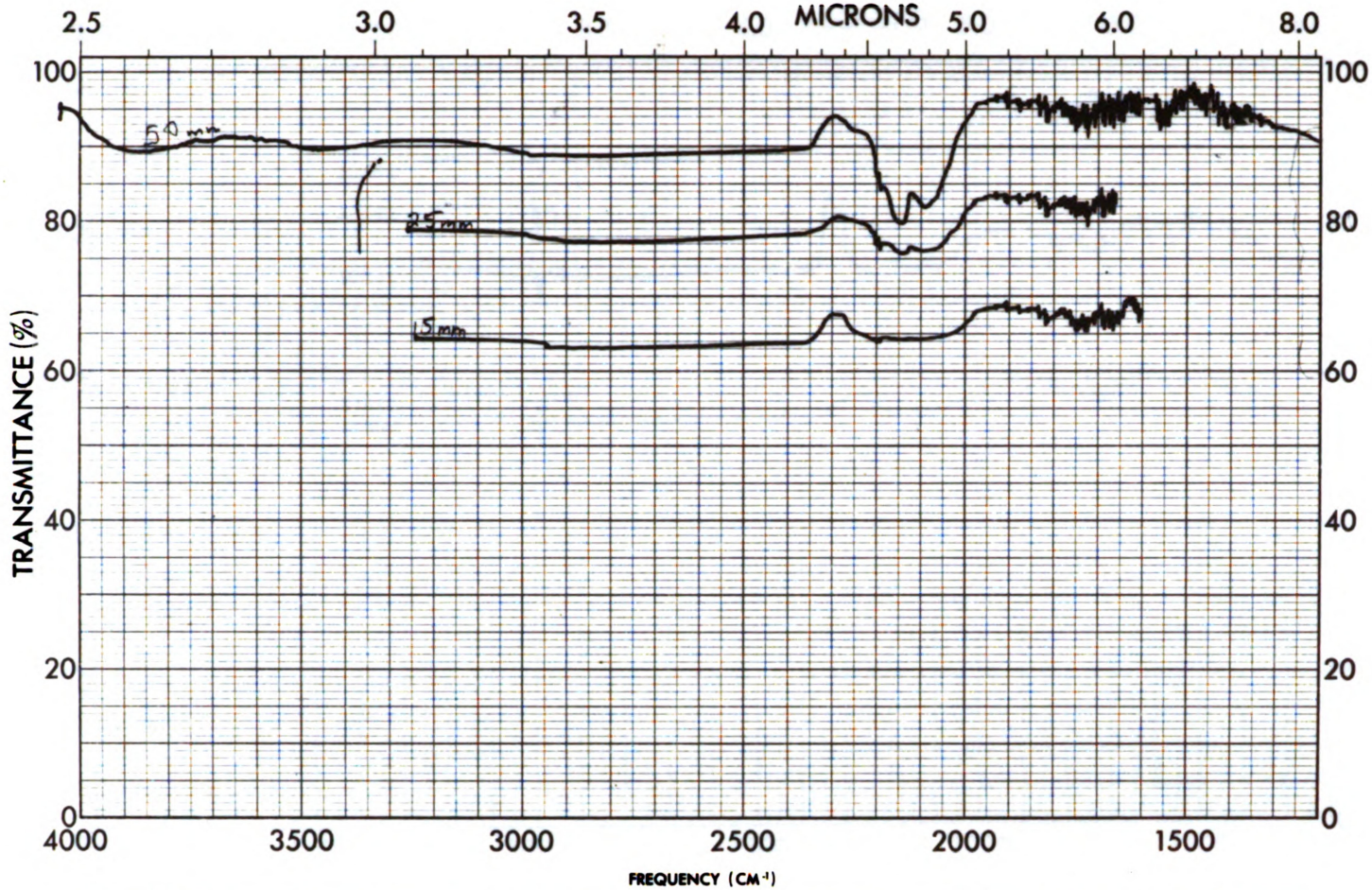

SAMPLE H_2/CO 4/1 NO PLASMA ORIGIN SOLVENT	INFARED SPECTRA 4	SCAN SPEED FAST SLIT N	OPERATOR MCH DATE 3-6-73 REMARKS

PART NO. 337-1203

PERKIN-ELMER ®

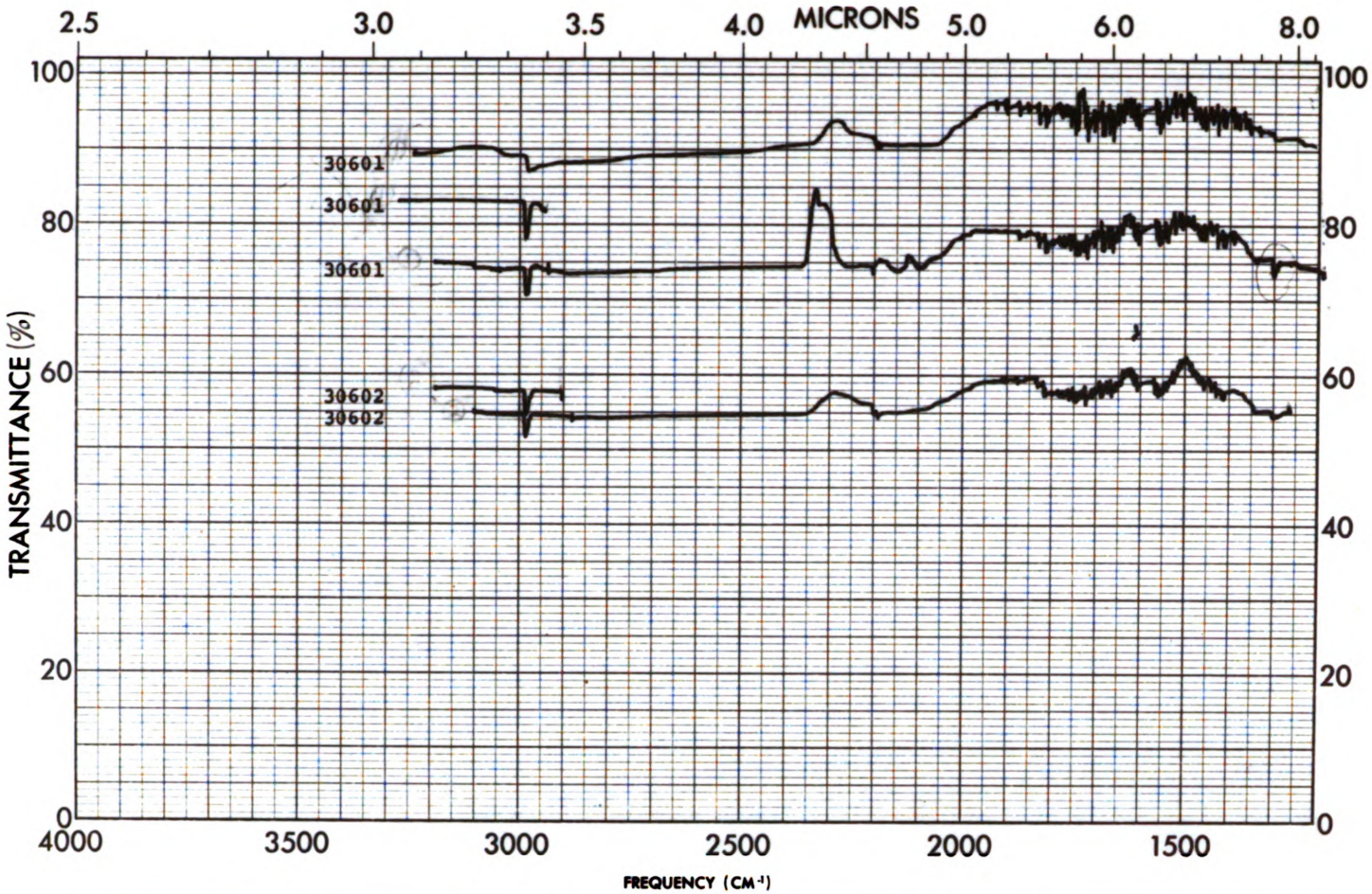

SAMPLE 4:1 H_2/CO WITH PLASMA	INFARED SPECTRA 5	SCAN SPEED SLOW	OPERATOR MCH/RLH
ORIGIN		SLIT N	DATE 3-6-73
SOLVENT		REMARKS	

PART NO. 337-1203

PERKIN-ELMER ®

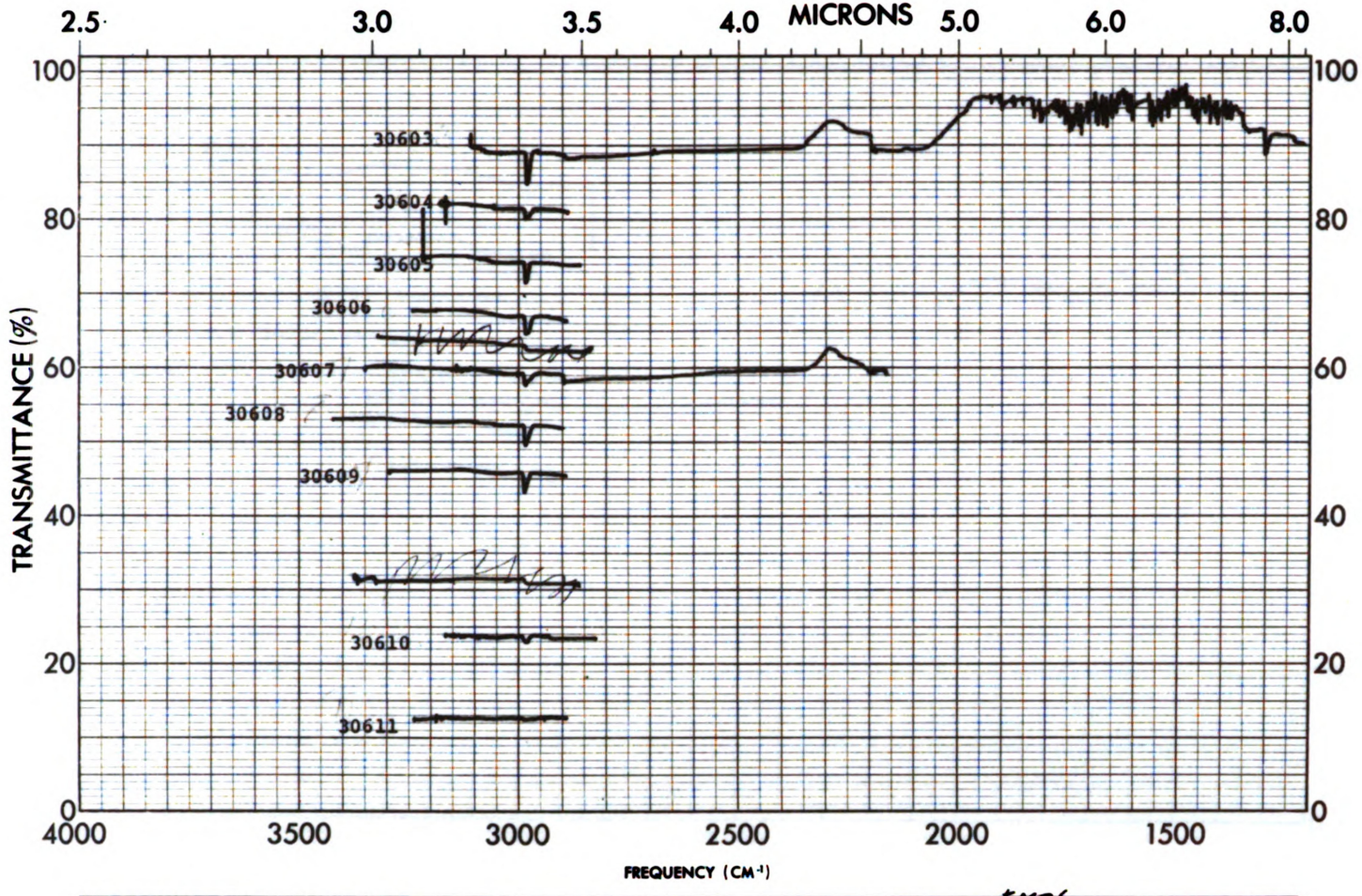

SAMPLE 4:1 H_2/CO WITH PLASMA REACTOR	INFARED SPECTRA 6	SCAN SPEED FAST/SLOW	OPERATOR MCM/ALM
ORIGIN		SLIT	DATE 3-5-23
SOLVENT		REMARKS	

PART NO. 337-1203

PERKIN-ELMER ®

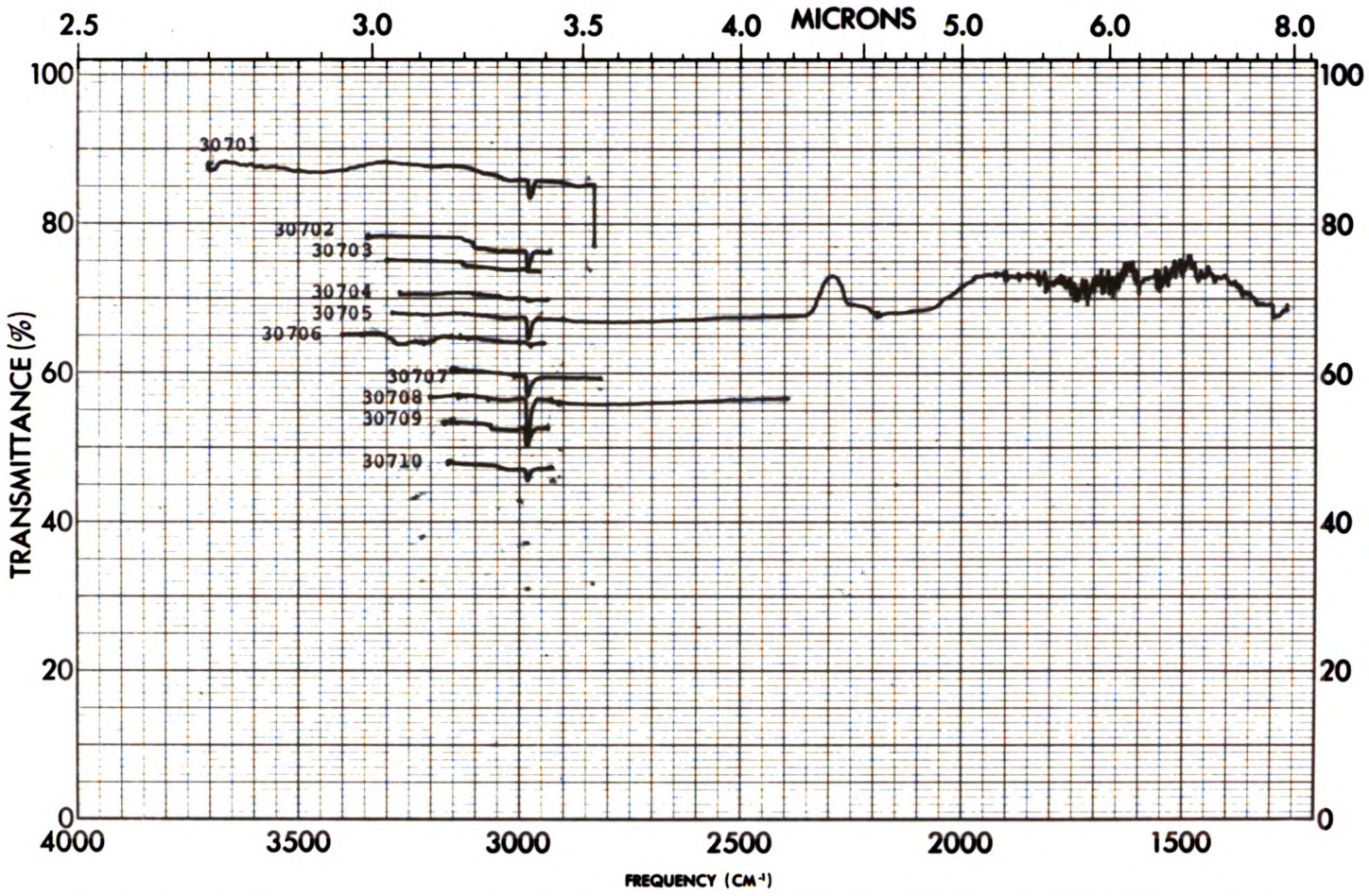

SAMPLE 4:1 H_2/CO PASSED THRU PLASMA REACTOR	INFARED SPECTRA 8	SCAN SPEED SLOW SLIT N	OPERATOR RLH DATE 8-7-73
ORIGIN		REMARKS CH_4 band AT ~3000 cm^{-1}	
SOLVENT			

PART NO. 337-1203

PERKIN-ELMER

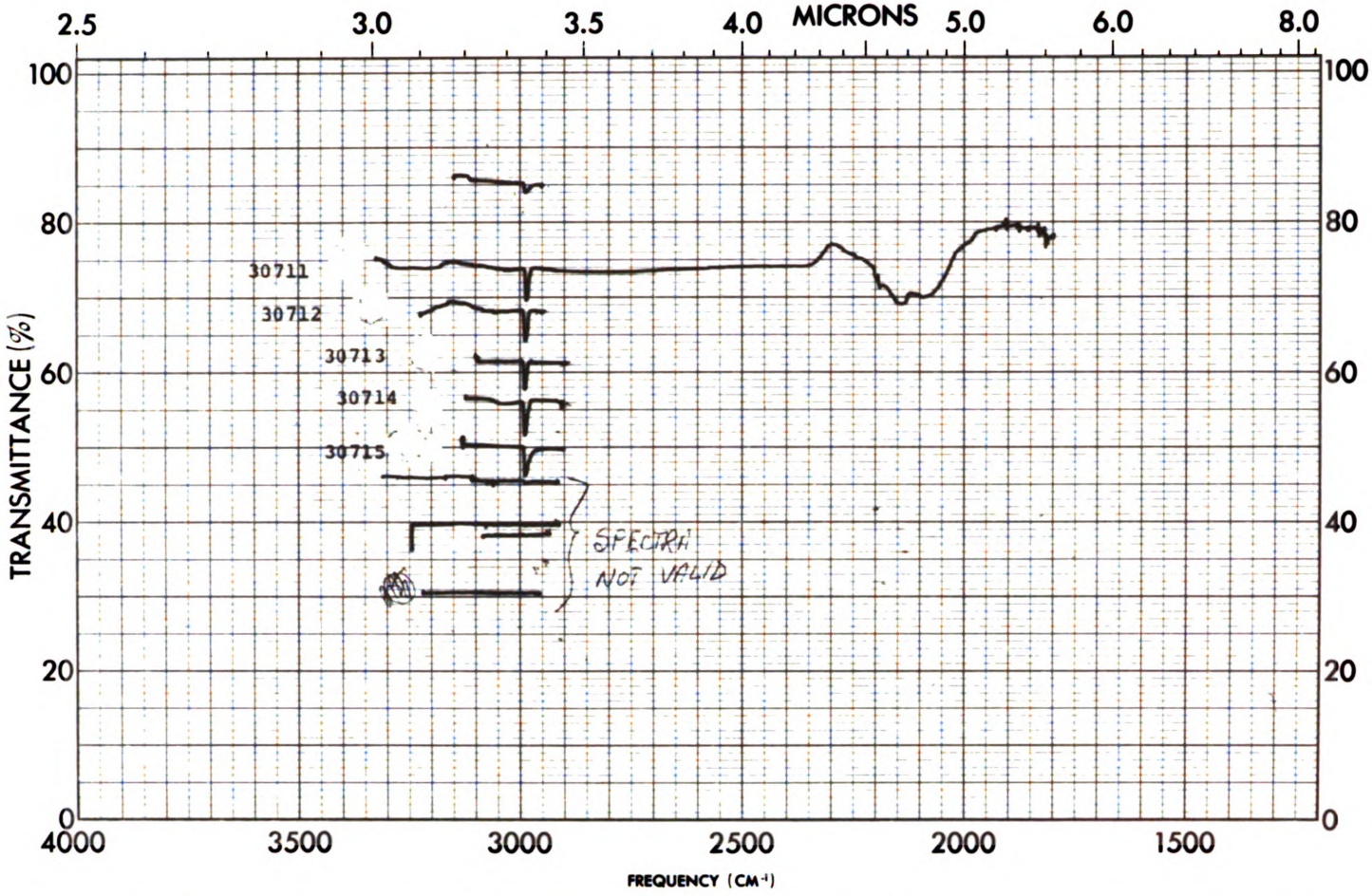

SAMPLE 4/1 H_2/CO IN PLASMA REACTOR	INFARED SPECTRA 9	SCAN SPEED SLOW	OPERATOR RLH
		SLIT IV	DATE 3-7-73
ORIGIN		REMARKS	
SOLVENT			

PART NO. 337-1203

PERKIN-ELMER ®

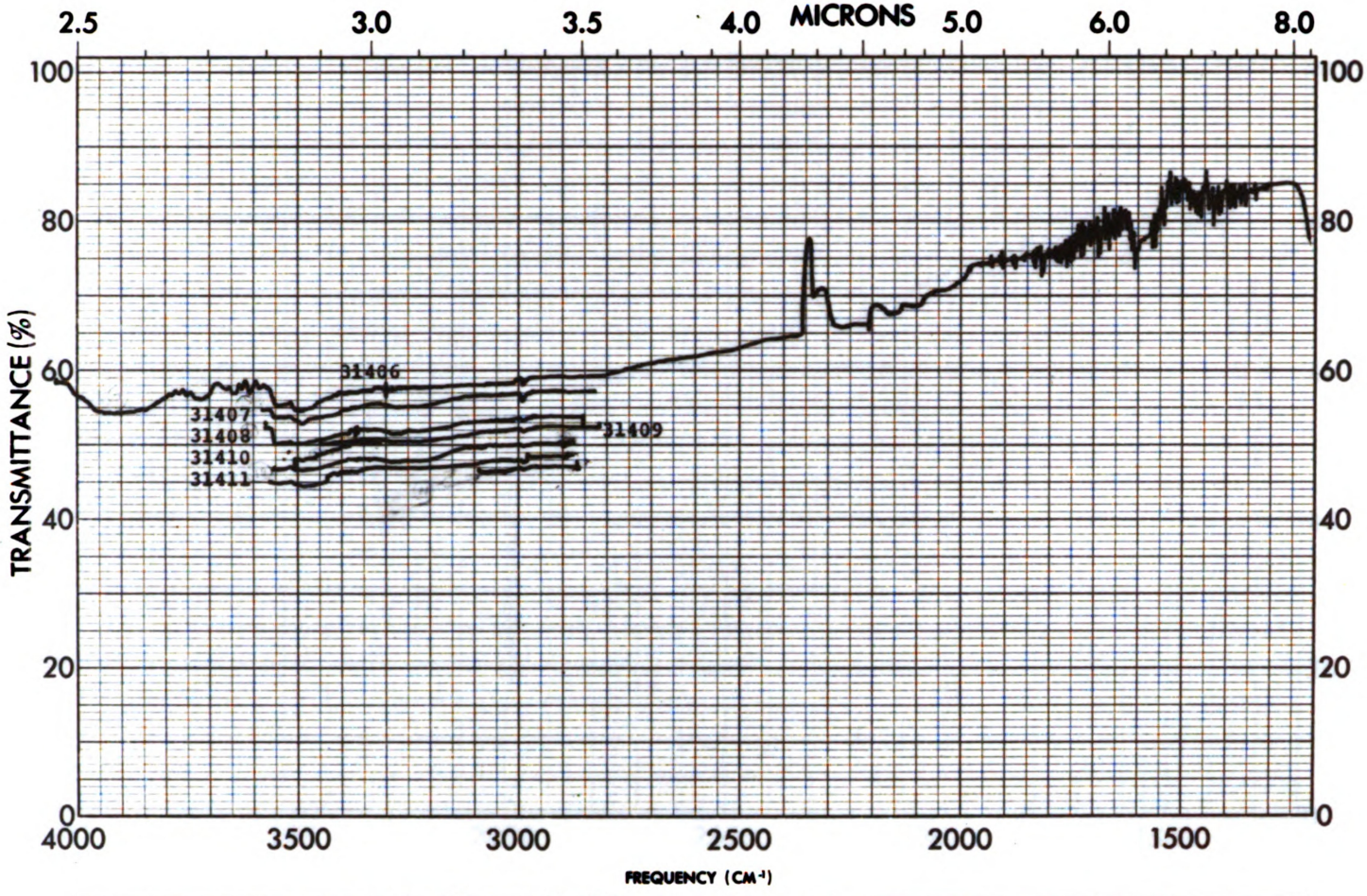

SAMPLE 1:1 Ho/Co Feed	INFARED SPECTRA 23	SCAN SPEED 5/1000	OPERATOR HCP
ORIGIN		SLIT N	DATE 03/14/'22
SOLVENT		REMARKS H2O Dry Ice trap	

PART NO. 337-1203

PERKIN-ELMER ®

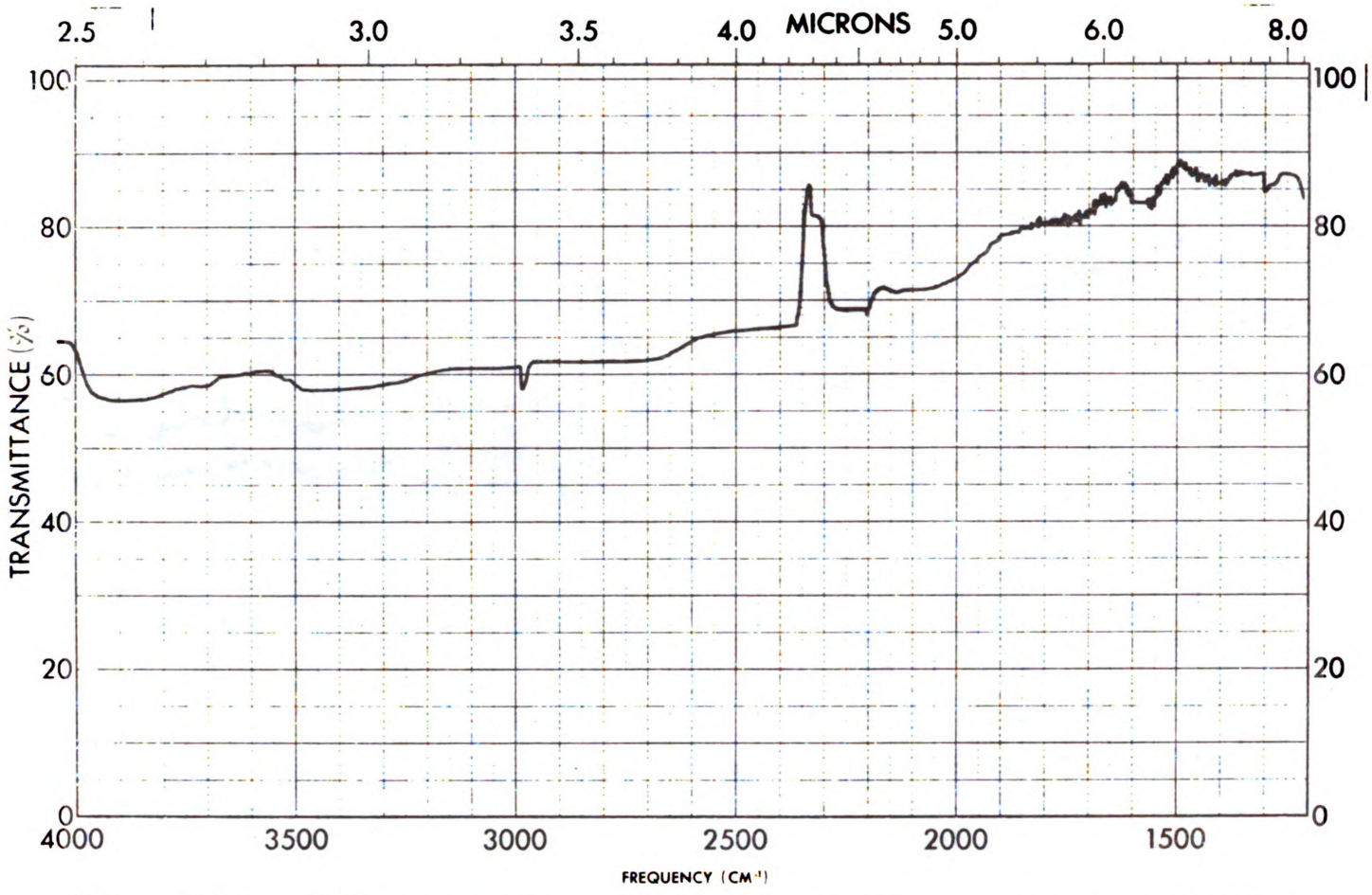

SAMPLE [illegible] IR calibration	INFARED SPECTRA 17	SCAN SPEED Slow	OPERATOR
ORIGIN		SLIT N	DATE 03/12/'73
SOLVENT		REMARKS 10 mm liq	

PART NO. 337-1203

PERKIN-ELMER®

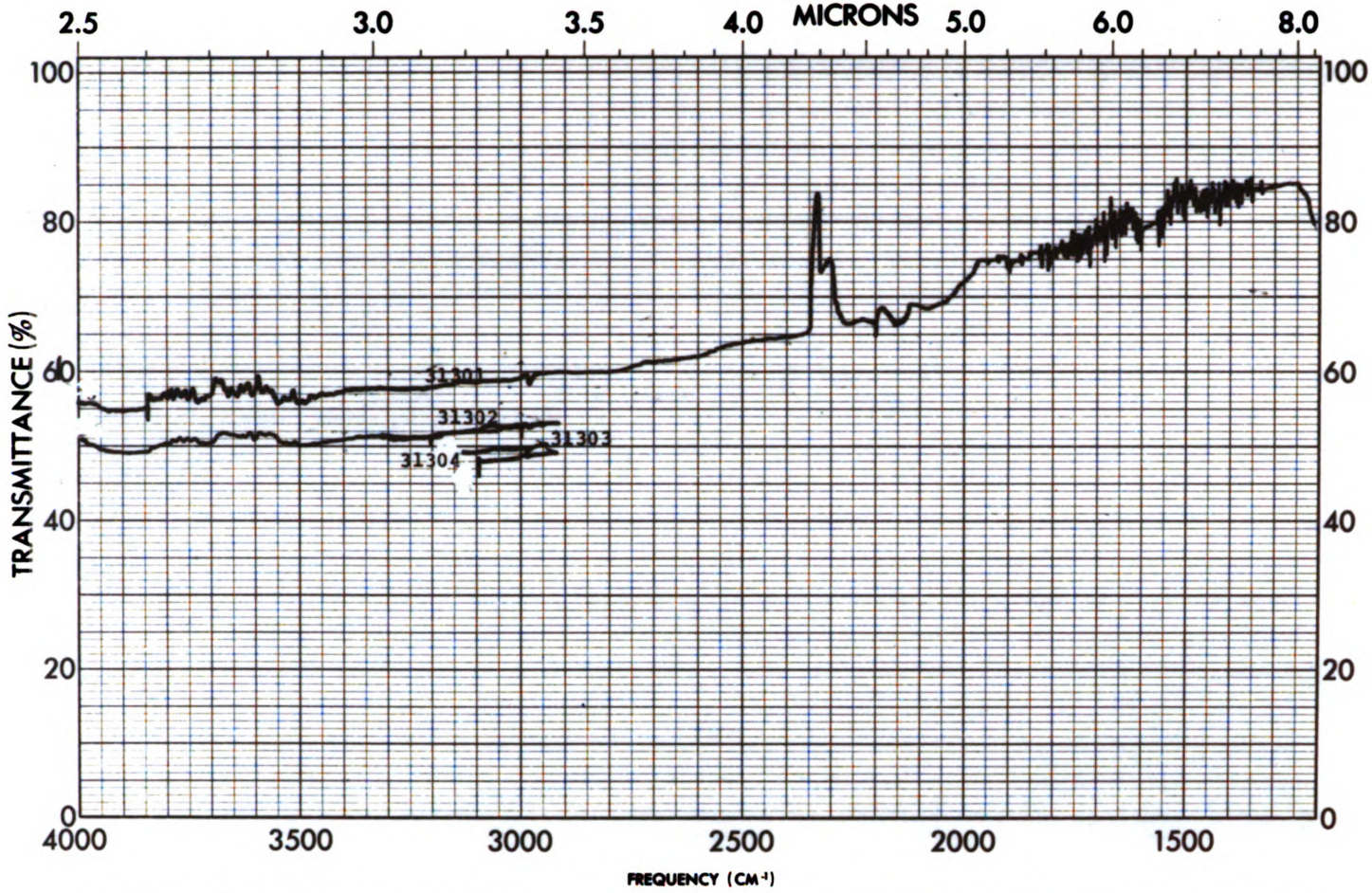

SAMPLE 1:1 H_2/CO SAMPLE IN PLASMA REACTOR ORIGIN SOLVENT	INFARED SPECTRA 19	SCAN SPEED SLOW SLIT N	OPERATOR RLH DATE 3-13-73
		REMARKS CH_4 ~ 3000 cm^{-1} $CH \div CH$ 3300 cm^{-1}	

PART NO. 337-1203

PERKIN-ELMER ®

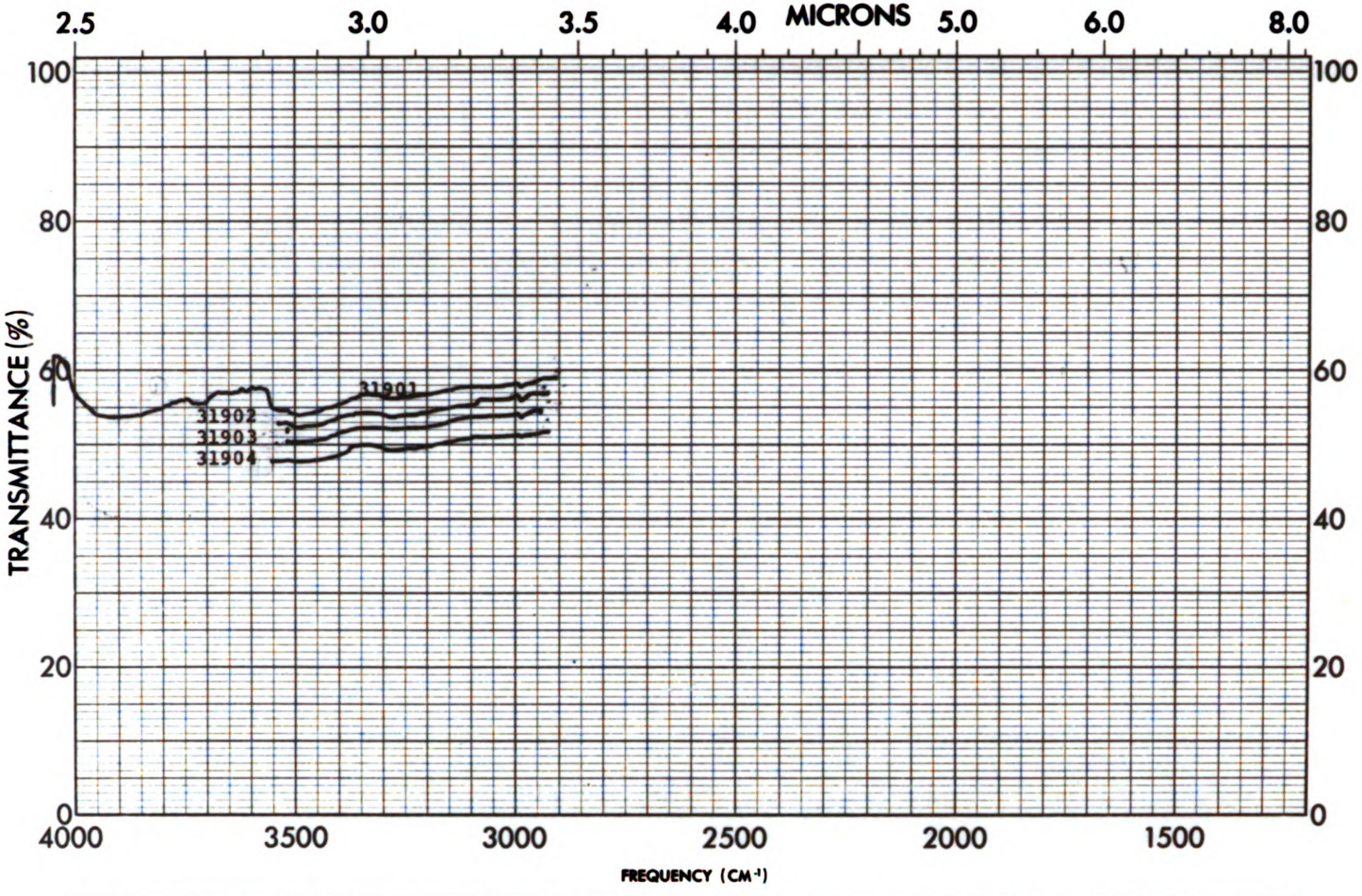

SAMPLE 4:1 H_2/CO	INFARED SPECTRA 26	SCAN SPEED Slow	OPERATOR
		SLIT N	DATE 03/19/73
ORIGIN		REMARKS 15 mm Hg P3 on/min	
SOLVENT		4% Dry Ice	

PART NO. 337-1203

PERKIN-ELMER

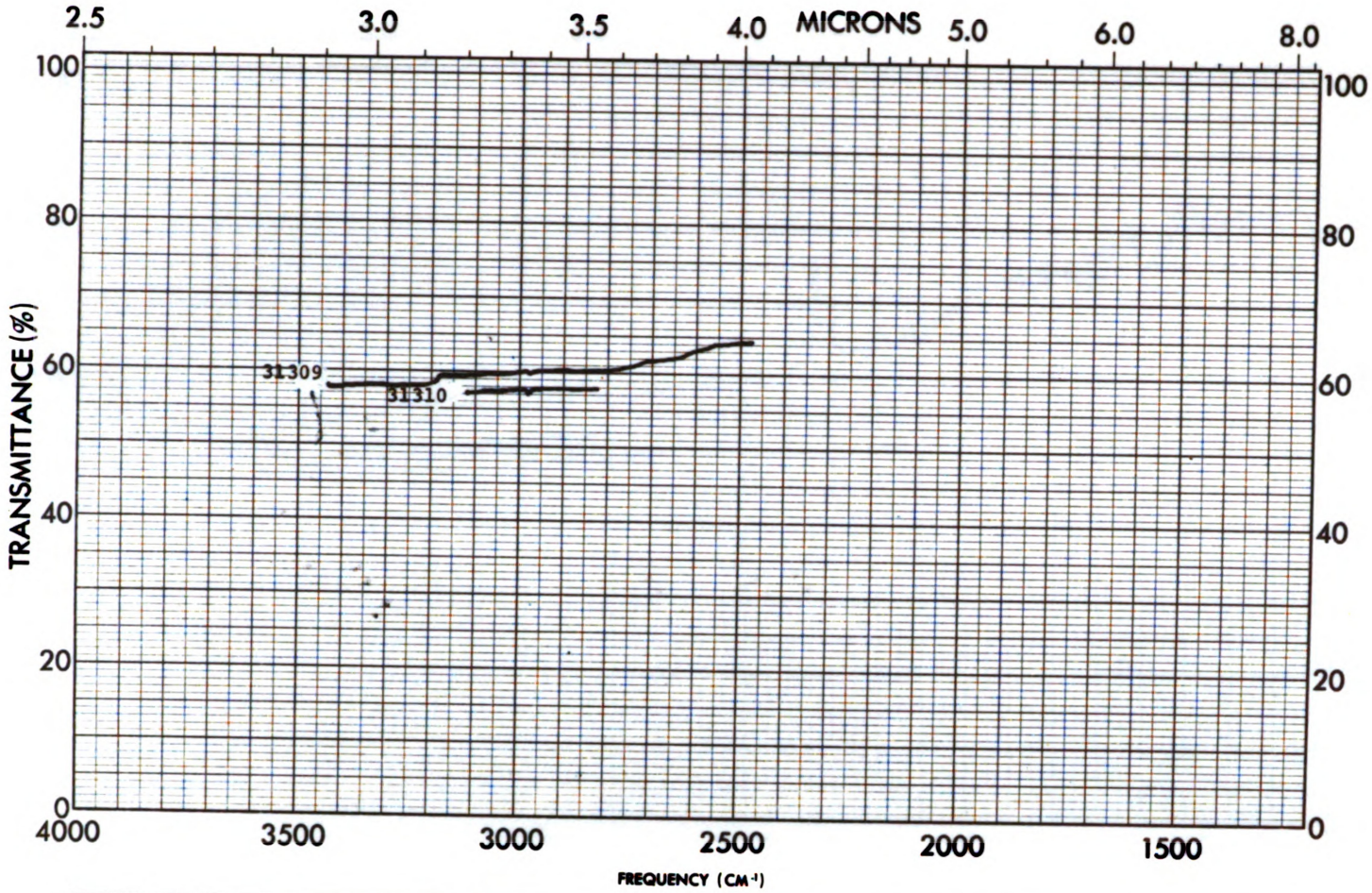

SAMPLE 1:1 H_2/CO	INFARED SPECTRA 21	SCAN SPEED 3400	OPERATOR ERH
ORIGIN		SLIT N	DATE 3-13-73
SOLVENT		REMARKS	

PART NO. 337-1203

PERKIN-ELMER ®

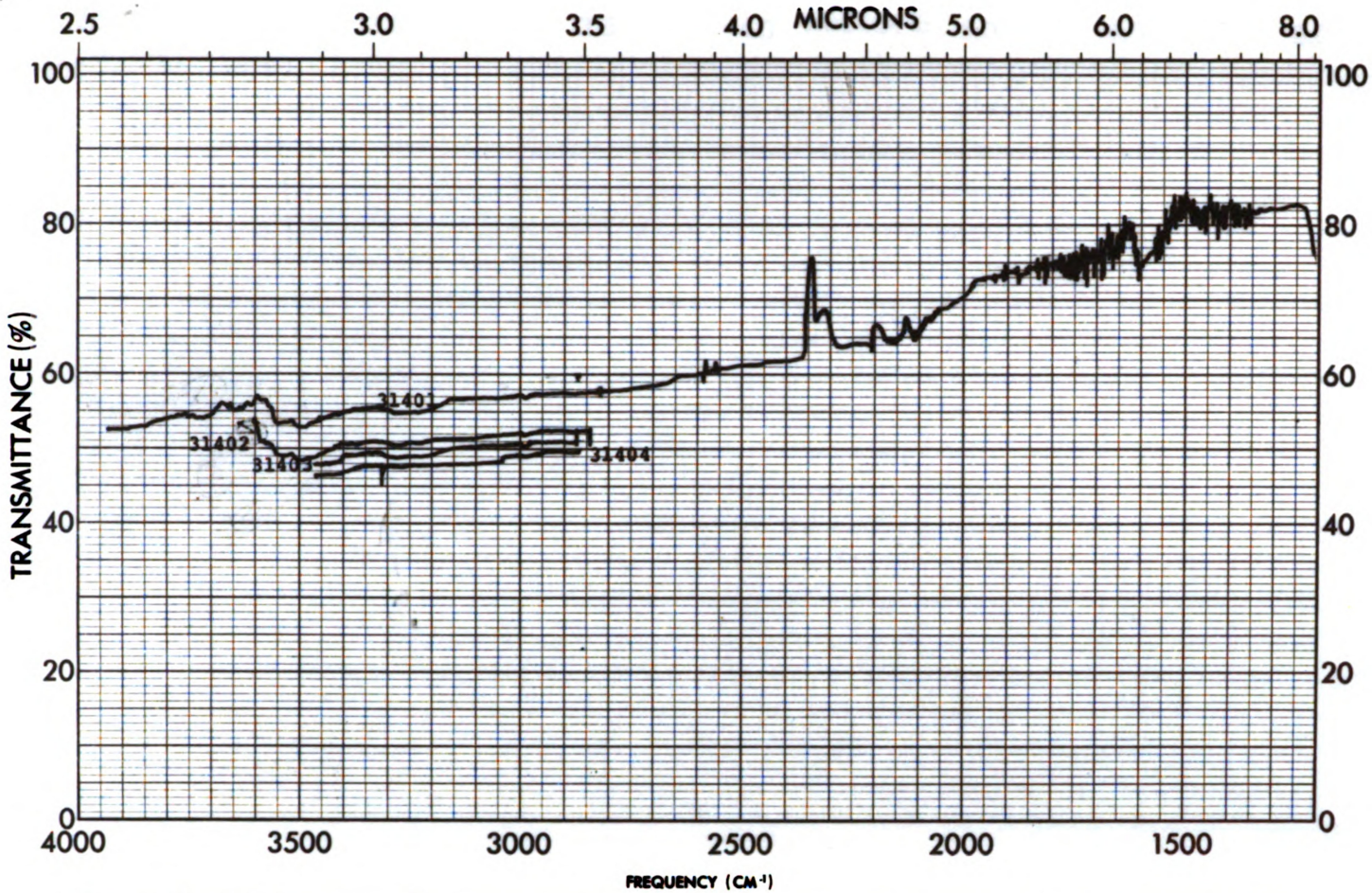

SAMPLE 1:1 Hy/Co Feed	INFARED SPECTRA 22	SCAN SPEED Slow	OPERATOR HCP
		SLIT N	DATE 03/14/73
ORIGIN		REMARKS 4/0 Dry Ice.	
SOLVENT			

PART NO. 337-1203

PERKIN-ELMER ®

APPENDIX B

Residence Time Computer Program

```
      PROGRAM PLASMA (OUTPUT)
      PRINT 40
   40 FORMAT (1H1,5X,*RESIDENCE TIME*5X*PRESSURE*2X*ROTAM
     1ETER FLOW*2X*PLASMA LENGTH*/SEC*13X*MM HG*7X*CC/MIN*
     112X*CM*)
   50 FORMAT (4F15.2)
      PI=3.14  $ DIA=2.54 $ DL=13.8*J=0
   30 PRESS=5.
   20 TAU=0.0
      V=PI*(DIA**2)*DL/4.
      DO 10 I=1,30
      TAU=TAU+.05
      FREAC=(V/TAU)*60.
      FROTA=FREAC*(PRESS/760.)*530./1260.
      PRINT 50,TAU,PRESS,FROTA,DL
      J=J+1
      IF(J.EQ.50)PRINT 40
      IF(J.EQ.50)  J=0
   10 CONTINUE
      PRESS=PRESS+ 5.0
      IF(PRESS.LT.35.) GO TO 20
      END
```

RESIDENCE TIME SEC	PRE... MM ...	...TER ... CC/MI...	... LE... CM
.05	5.00	[illegible]	13.80
.10	5.00	116.05	13.80
.15	5.00	77.36	13.80
.20	5.00	58.02	13.80
.25	5.00	46.42	13.80
.30	5.00	38.68	13.80
.35	5.00	33.16	13.80
.40	5.00	29.01	13.80
.45	5.00	25.79	13.80
.50	5.00	23.21	13.80
.55	5.00	21.10	13.80
.60	5.00	19.34	13.80
.65	5.00	17.85	13.80
.70	5.00	16.58	13.80
.75	5.00	15.47	13.80
.80	5.00	14.51	13.80
.85	5.00	13.65	13.80
.90	5.00	12.89	13.80
.95	5.00	12.22	13.80
1.00	5.00	11.60	13.80
1.05	5.00	11.05	13.80
1.10	5.00	10.55	13.80
1.15	5.00	10.09	13.80
1.20	5.00	9.67	13.80
1.25	5.00	9.28	13.80
1.30	5.00	8.93	13.80
1.35	5.00	8.60	13.80
1.40	5.00	8.29	13.80
1.45	5.00	8.00	13.80
1.50	5.00	7.74	13.80
.05	10.00	464.18	13.80
.10	10.00	232.09	13.80
.15	10.00	154.73	13.80
.20	10.00	116.05	13.80
.25	10.00	92.84	13.80
.30	10.00	77.36	13.80
.35	10.00	66.31	13.80
.40	10.00	58.02	13.80
.45	10.00	51.58	13.80
.50	10.00	46.42	13.80
.55	10.00	42.20	13.80
.60	10.00	38.68	13.80
.65	10.00	35.71	13.80
.70	10.00	33.16	13.80
.75	10.00	30.95	13.80
.80	10.00	29.01	13.80
.85	10.00	27.30	13.80
.90	10.00	25.79	13.80
.95	10.00	24.43	13.80
1.00	10.00	23.21	13.80

RESIDENCE TIME SEC	PRESS [illegible]	WATER FLOW (GPM)	[illegible]
1.05	[illegible]	[illegible]	[illegible]
1.10	[illegible]	[illegible]	13.80
1.15	[illegible]	[illegible]	13.80
1.20	[illegible]	19.34	13.80
1.25	[illegible]	18.57	13.80
1.30	[illegible]	17.85	13.80
1.35	[illegible]	17.19	13.80
1.40	15.00	16.58	13.80
1.45	15.00	16.01	13.80
1.50	15.00	15.47	13.80
.05	[illegible]	[illegible]	13.80
.10	[illegible]	[illegible]	13.80
.15	[illegible]	[illegible]	13.80
.20	15.00	174.07	13.80
.25	15.00	139.25	13.80
.30	15.00	116.05	13.80
.35	15.00	99.47	13.80
.40	15.00	87.03	13.80
.45	15.00	77.36	13.80
.50	15.00	69.63	13.80
.55	15.00	63.30	13.80
.60	15.00	58.02	13.80
.65	15.00	53.56	13.80
.70	15.00	49.73	13.80
.75	15.00	46.42	13.80
.80	15.00	43.52	13.80
.85	15.00	40.96	13.80
.90	15.00	38.68	13.80
.95	15.00	36.65	13.80
1.00	15.00	34.81	13.80
1.05	15.00	33.16	13.80
1.10	15.00	31.65	13.80
1.15	15.00	30.27	13.80
1.20	15.00	29.01	13.80
1.25	15.00	27.85	13.80
1.30	15.00	26.78	13.80
1.35	15.00	25.79	13.80
1.40	15.00	24.87	13.80
1.45	15.00	24.01	13.80
1.50	15.00	23.21	13.80
.05	20.00	928.37	13.80
.10	20.00	464.18	13.80
.15	20.00	309.46	13.80
.20	20.00	232.09	13.80
.25	20.00	185.67	13.80
.30	20.00	154.73	13.80
.35	20.00	132.62	13.80
.40	20.00	116.05	13.80
.45	20.00	103.15	13.80
.50	20.00	92.84	13.80

RESIDENCE TIME SEC	[illegible]	[illegible] CC/MIN.	PLASMA LENGTH CM
.55	20.[illegible]	84.40	13.80
.60	20.00	77.36	13.80
.65	20.00	71.41	13.80
.70	20.00	66.31	13.80
.75	20.00	61.89	13.80
.80	20.00	58.02	13.80
.85	20.00	54.61	13.80
.90	20.00	51.58	13.80
.95	20.00	48.86	13.80
1.00	20.00	46.42	13.80
1.05	20.00	44.21	13.80
1.10	20.00	42.20	13.80
1.15	20.00	40.36	13.80
1.20	20.00	38.68	13.80
1.25	20.00	37.13	13.80
1.30	20.00	35.71	13.80
1.35	20.00	34.38	13.80
1.40	20.00	33.16	13.80
1.45	20.00	32.01	13.80
1.50	20.00	30.95	13.80
.05	25.00	1160.46	13.80
.10	25.00	580.23	13.80
.15	25.00	386.82	13.80
.20	25.00	290.11	13.80
.25	25.00	232.09	13.80
.30	25.00	193.41	13.80
.35	25.00	165.78	13.80
.40	25.00	145.06	13.80
.45	25.00	128.94	13.80
.50	25.00	116.05	13.80
.55	25.00	105.50	13.80
.60	25.00	96.70	13.80
.65	25.00	89.27	13.80
.70	25.00	82.89	13.80
.75	25.00	77.36	13.80
.80	25.00	72.53	13.80
.85	25.00	68.26	13.80
.90	25.00	64.47	13.80
.95	25.00	61.08	13.80
1.00	25.00	58.02	13.80
1.05	25.00	55.26	13.80
1.10	25.00	52.75	13.80
1.15	25.00	50.45	13.80
1.20	25.00	48.35	13.80
1.25	25.00	46.42	13.80
1.30	25.00	44.63	13.80
1.35	25.00	42.98	13.80
1.40	25.00	41.44	13.80
1.45	25.00	40.02	13.80
1.50	25.00	38.68	13.80

RESIDENCE TIME SEC	PRESSURE MM HG	[illegible] FLOW CC/MIN	PLASMA LENGTH CM
.05	[illegible]	[illegible]	13.80
.10	30.00	696.27	13.80
.15	30.00	464.18	13.80
.20	30.00	348.14	13.80
.25	30.00	278.51	13.80
.30	30.00	232.09	13.80
.35	30.00	198.94	13.80
.40	30.00	174.07	13.80
.45	30.00	154.73	13.80
.50	30.00	139.25	13.80
.55	30.00	126.60	13.80
.60	30.00	116.05	13.80
.65	30.00	107.12	13.80
.70	30.00	99.47	13.80
.75	30.00	92.84	13.80
.80	30.00	87.03	13.80
.85	30.00	81.91	13.80
.90	30.00	77.35	13.80
.95	30.00	73.29	13.80
1.00	30.00	69.63	13.80
1.05	30.00	66.31	13.80
1.10	30.00	63.30	13.80
1.15	30.00	60.55	13.80
1.20	30.00	58.02	13.80
1.25	30.00	55.70	13.80
1.30	30.00	53.56	13.80
1.35	30.00	51.58	13.80
1.40	30.00	49.73	13.80
1.45	30.00	48.02	13.80
1.50	30.00	46.42	13.80